DIRECT MEASUREMENTS OF NITROUS ACID, NITROGEN DIOXIDE, AND FORMALDEHYDE IN AUTO EXHAUST BY DIFFERENTIAL OPTICAL ABSORPTION SPECTROSCOPY

CONTRACT NUMBER A9-118-30
CALIFORNIA AIR RESOURCES BOARD
Final Report

Principal Investigator

James N. Pitts, Jr.

Co-Investigators

Geoffrey W. Harris
Arthur M. Winer

STATEWIDE AIR POLLUTION RESEARCH CENTER
UNIVERSITY OF CALIFORNIA
RIVERSIDE, CALIFORNIA 92521

June 1982

ABSTRACT

Gaseous nitrous acid (HONO) has been identified and measured for the first time in samples of diluted and cooled exhaust gases taken from light duty motor vehicles (LDMV) with gasoline engines run in several modes on the ARB chassis dynamometer-constant volume sampling (CVS) facility at the Haagen-Smit Laboratory in El Monte. A unique, shortpath (3.6 m) UV-visible, differential optical absorption spectrometer (DOAS) developed specifically for this project was used to measure HONO levels ranging from nondetectable (< 0.05 ppm) up to several ppm. Nitrogen dioxide and formaldehyde levels were measured with this spectrometer concurrently. In one run with a high NO_x-emitting vehicle, a concentration of ~8 ppm of HONO was measured in a sample bag filled according to established procedures with dilute exhaust gases. Preliminary studies suggest that the HONO may not be present in the hot, concentrated exhaust gases immediately leaving the tailpipe, but is formed downstream in the CVS train upon dilution and cooling, possibly by heterogeneous wall processes.

Knowledge of ambient HONO concentrations, and their sources, can be a critical input to models of photochemical oxidant production in California's congested urban and suburban areas because HONO is a key initiator in the chain processes leading to ozone formation in irradiated HC-NO_x systems. Our initial results suggest that, after dilution and cooling with ambient air, LDMV exhaust emissions may contribute to the relatively high levels of ambient HONO we have recently observed with a longpath DOAS system over a freeway interchange near downtown Los Angeles (DTLA). Additionally, the unequivocal, spectroscopic measurement of ~8 ppm HONO in a sample bag filled with diluted LDMV exhaust according to standard practices not only has significant implications for current exhaust analysis methodologies, but also for studies of health effects arising from the exposure of animals to diluted exhaust gases from LDMV run on chassis dynamometers.

TABLE OF CONTENTS

ACKNOWLEDGMENTS

We gratefully acknowledge the support provided for this research program by the staff of the ARB Haagen-Smit Laboratory. The Chief, Mr. G. C. Haas, and Mr. Al Donnelly, Supervising MVPC Engineer, were most cooperative. Also Mr. Frank Bonamassa, Supervising Air Resources Engineer, and Mr. Paul Newmark, Senior Air Resources Engineer of his staff, provided access to facilities and helpful advice on their use, without which our research could not have been performed.

SAPRC research staff members Dr. Jack Treacy, Dr. Uli Platt, Mr. Nick Miller and Mr. Alan Echt were involved in much of the instrument development and data acquisition while Ms. C. J. Ranck, Ms. I. M. Minnich, Ms. M. R. Peterson and Ms. Y. A. Katzenstein provided valuable assistance in the preparation of this document.

This report was submitted in fulfillment of Contract Number A9-118-30, "Direct Measurements of Nitrous Acid, Nitrogen Dioxide, and Formaldehyde in Auto Exhaust by Differential Optical Absorption Spectroscopy" by the Statewide Air Pollution Research Center, University of California, Riverside, under the sponsorship of the California Air Resources Board. Experimental work was completed as of September 1, 1981.

The statements and conclusions in this report are those of the Contractor and not necessarily those of the California Air Resources Board. The mention of commercial products, their source, or their use in connection with material reported herein, is not to be construed as either an actual or implied endorsement of such products.

LIST OF FIGURES

LIST OF TABLES

I. PROJECT SUMMARY

Introduction and Statement of the Problem. The gas phase photooxidation of organics in the presence of nitrogen oxides (NO_x) in the polluted troposphere is a highly complex chain reaction which results in the formation of ozone and a variety of criteria and noncriteria pollutants. It is initiated by the attack of hydroxyl radicals (OH) on organic compounds (RH), followed by a long series of elementary free radical reactions. Nitrous acid vapor can be a critical pollutant in this process.

Recent spectroscopic studies of ambient air over a major freeway intersection (Interstate 10 and California State 7) near downtown Los Angeles (DTLA) by Statewide Air Pollution Research Center (SAPRC) researchers using a novel, longpath differential optical absorption spectrometer (DOAS) system originally developed by German scientists (Perner and Platt 1979), have shown levels up to ~8 ppb (one part in 10^9) HONO (Harris et al. 1982). Accompanying model calculations predict that at these concentrations photolysis of HONO by sunlight (Equation 1) represents a major early morning source of OH radicals (Harris et al. 1982):

$$HONO + h\nu \ (\leq 400 \text{ nm}) \rightarrow OH + NO. \qquad (1)$$

In addition to its impact on photochemical oxidant production, HONO in ambient air could have possible adverse health effects. For example, in simulated atmospheres containing ambient levels of NO_x (and presumably HONO), secondary amines react rapidly in the dark to form, in part, highly carcinogenic gaseous nitrosamines (Pitts et al. 1978). Furthermore, in sunlight these are subsequently photooxidized to nitramines (Tuazon et al. 1978). At least one of these (dimethylnitramine) is also an animal carcinogen (Druckrey et al. 1961, Goodall and Kennedy 1976). The possibility must also be considered that the direct inhalation of HONO could form nitrosamines *in vivo*.

Research Objectives:

- To design, construct and test a new shortpath (~3.6 m) UV/visible, DOAS system which could be used to determine whether or not HONO was present as a gaseous "primary" pollutant in dilute, automobile exhaust.

[Note that we define "primary" pollutant as a chemical species either present in the hot exhaust gases as they leave the tailpipe (e.g., formaldehyde) or one that is formed very rapidly on dilution and cooling of the exhaust gases in the atmosphere.]

- In conjunction with the ARB chassis dynamometer-CVS facilities at the Haagen-Smit Laboratories, El Monte, make initial measurements of the concentrations of HONO, NO_2 and HCHO in diluted auto exhaust taken at two downstream points in the CVS system for a range of vehicle types and engine operating conditions.

- To make initial estimates of the possible contribution of LDMV to ambient HONO levels, as a result of HONO being present in their exhaust gases, or being formed very rapidly following their dilution and cooling in the atmosphere.

Summary of Results. Overall we have designed, constructed and tested a new shortpath DOAS system (Figure 1) and our initial studies have resulted in:

- The first positive spectroscopic identification of gaseous HONO in diluted auto exhaust, and

- The demonstration of the feasibility of this technique for concurrent, direct, on line HCHO and NO_2 measurements.

The new shortpath DOAS system developed and employed for this program (Figure 1) utilizes white light from a high pressure Xe arc lamp (75 W) collimated into a parallel beam by a spherical mirror. The beam is transmitted through a special sample cell (3.6 m pathlength) designed for dilute exhaust gases (and particles), to a point where it is received by a Newtonian telescope and focused on the entrance slit of a 0.3 meter McPherson spectrograph equipped with a 600 groove mm^{-1} grating (dispersion ~4 nm mm^{-1}). A rotating thin metal disc (20 cm diameter) with radial slits (100 μm wide, ~10 mm spacing) is placed in the exit focal plane; thus a segment of the spectrum is scanned repetitively in any spectral region. Just before reaching the section to be scanned, each slit passes through an infrared light barrier so that the spectral position of the slit is defined. By keeping the rotation of the disk constant (to within 0.5%), the spectral scans of all the slits can be accurately superimposed. The light intensity passing through the slit is monitored by a

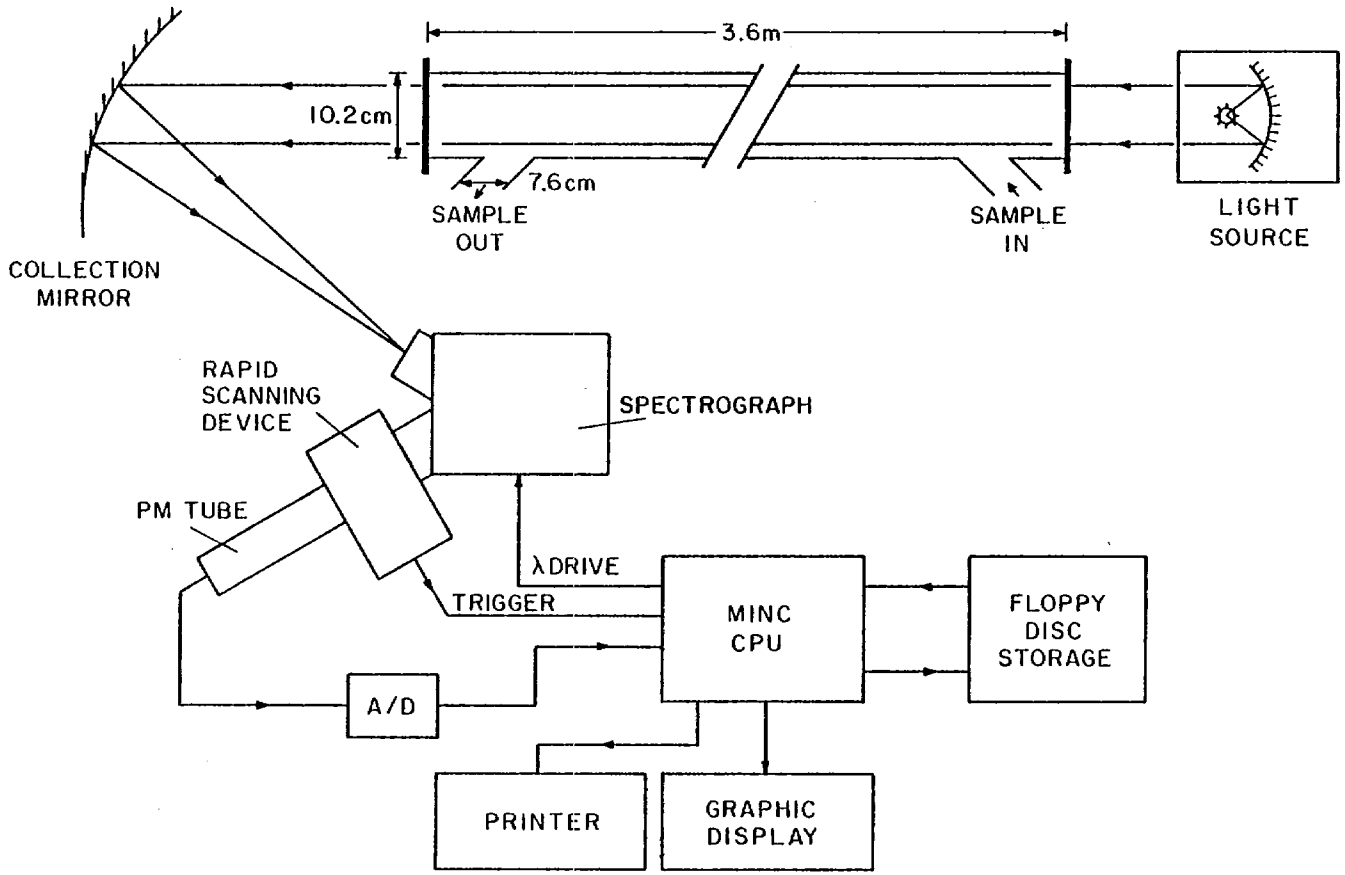

Figure 1. The shortpath differential optical absorption spectrometer (DOAS) system.

photomultiplier (EMI 9659Q), and the signal is averaged for about 25 μsec. It is then digitized (12 bits) and stored by a computer (DEC MINC-11/23). The computer is used to average the scans and to manipulate the data in spectral deconvolution and calculation of optical densities.

In the majority of the experiments, the effluent at point C (Figure 2), which consisted of diluted, cooled auto exhaust from the dynamometer-CVS facility, was directed through the flow tube-type sample cell and spectroscopically analyzed. In one experiment the contents of a sample bag filled at point B (Figure 2) according to the standard procedure were flushed into the flow cell and analyzed. The DOAS instrument and the operating procedures are described in detail in Section II.

This shortpath DOAS system is capable of measuring HONO in diluted auto exhaust with a detection limit of ~50 ppb. The detection limit for HCHO is dependent on the amount of NO_2 in the sample and the experimental configuration. In these runs, the limit was ~0.3 ppm in the best cases. However, the ultimate detection limit for HCHO, another important initiator of photochemical air pollution as well as a strong, gas phase animal carcinogen, can be lowered by straightforward changes in the experimental procedure (and, in principle, data on acrolein levels could also be obtained). Such changes would have reduced the number of HONO measurements in the various test vehicles and were therefore not implemented in this first year program. These changes would make an interesting element in a future program.

The use of the shortpath DOAS technique in the analysis of complex gaseous mixtures for "trace" components such as HONO now appears to offer several major advantages over conventional analytical methods. These include rapid, on-line data acquisition and reduction, and the potential for making multi-component measurements of trace species with a high degree of specificity and excellent sensitivities. In contrast, wet chemical methods, and certain other off-line analyses for "trace" pollutant species [either in the atmosphere at the sub-ppb to ppm range, or in auto exhaust at the ppm to percent range], can suffer from a number of difficulties. Thus, if a specific procedure is required for each of several species it is unlikely that rapid, simultaneous multicomponent analyses will be possible. Also, the time required for analyses or sample

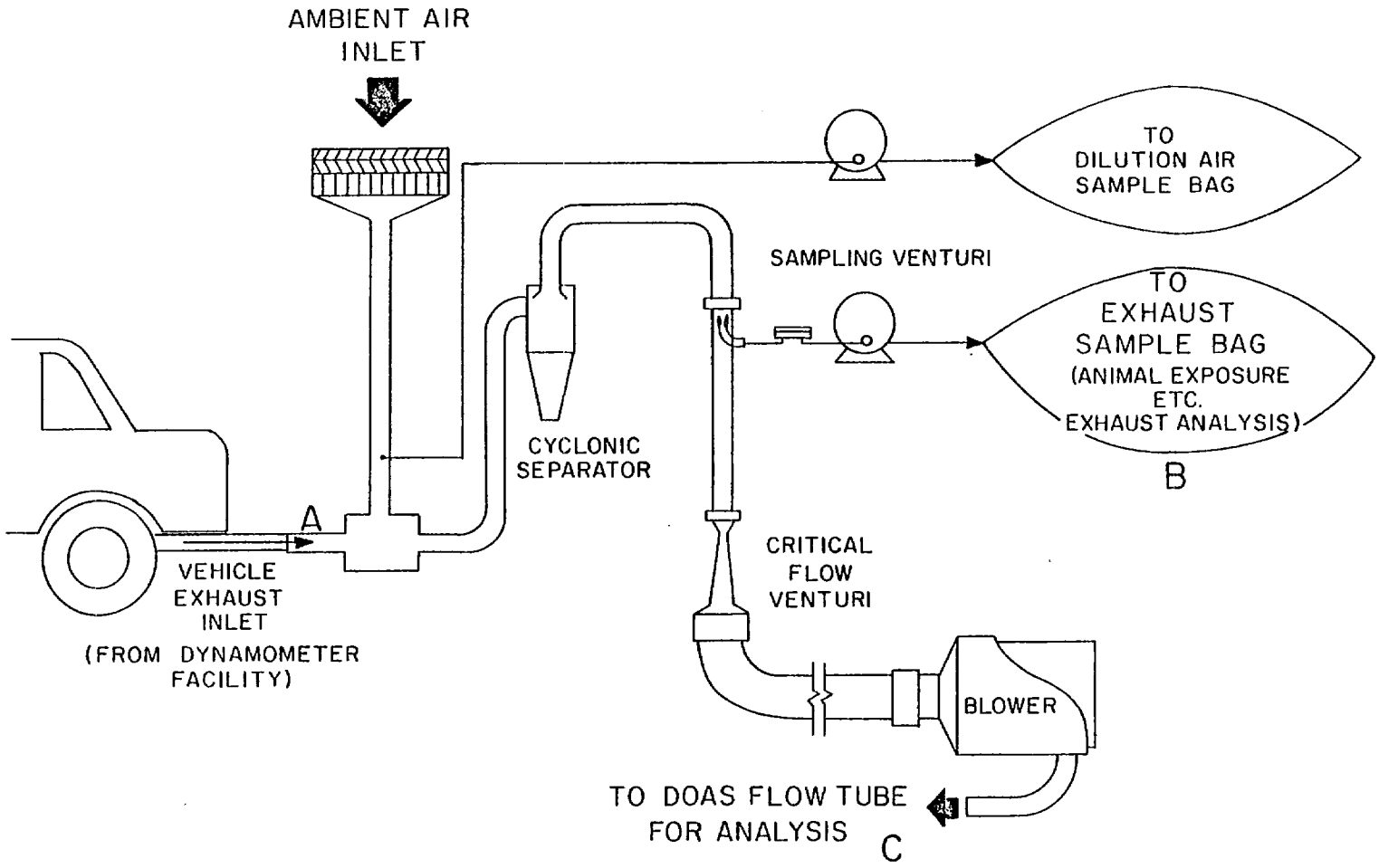

Figure 2. Dynamometer-constant volume sampler (CVS) equipment used in conjunction with the DOAS system. Exhaust samples were obtained at points B or C for spectroscopic analysis.

collection may be long compared to the characteristic times for changes in the concentrations of species during, for example, standard driving cycles, and hence only "averaged" rather than dynamic information would be available. Finally, the problem of interferences among gas phase or particulate co-pollutants may be serious for many instrumental and wet chemical analyses.

Specific results obtained using the new DOAS system are summarized below:

- HONO has been unambiguously identified as a component both of the contents of a sample bag filled with LDMV exhaust according to standard procedure (point B, Figure 2), and of the effluent from the ARB-CVS apparatus (point C, Figure 2).

- Using the flow tube configuration (i.e., spectrometer cell) at point C, highly variable amounts of HONO [ranging from indetectable (< 50 ppb) to ~2.6 ppm] and NO_2, and highly variable ratios of $HONO/NO_2$ (ranging from ~0.0 to 0.43), have been observed in the effluent from the ARB-CVS system. The values depended on both the test vehicle and the operating mode.

- A sample bag filled using a dilution factor of 5.12 with the exhaust from a high NO_x-emitting, 1980 six-cylinder, 300 cubic inch Ford custom pickup operated in the standard highway driving cycle contained 8.5 ppm HONO and 67 ppm NO_2. ARB chemiluminescence analysis of the same sample determined 210 ppm NO_x, 141 ppm NO and 69 ppm NO_2 ($[NO_2]=[NO_x]-[NO]$). The ARB result of 69 ppm NO_2 was in good agreement with the DOAS value of 67 ppm. HONO comprised ~4% of the NO_x in the bag and was present at ~13% of the NO_2 concentration.

The probable occurrence of heterogeneous, physical (e.g., wall adsorption) and chemical processes on surfaces in the CVS system limits our present interpretation of the absolute values of HONO which were measured in these experiments. Thus much, and quite possibly all, of the HONO observed at point C may have been formed after the hot gases left the tailpipes of the vehicles and were cooled and diluted with air in the CVS train. Nevertheless, our initial data indicate that under freeway driving conditions significant levels of HONO could be formed in ambient air from

the rapid dilution and cooling of the exhaust gases. This hypothesis is currently being tested.

The observation of 8.5 ppm of nitrous acid in a sample bag filled (at point B) by recommended ARB/Federal procedures raises the possibility that exhaust samples collected by standard procedures in bags or in smog chambers and stored in the light for some period of time before analysis may be subject to considerable photochemical modifications. These could occur as a result of HONO photolysis (Equation 1) and subsequent reactions initiated by the OH radicals produced in the process.

The presence of significant levels of HONO in the bag sample taken at point B also has potentially significant implications for studies of the effects of dilute auto exhaust on the health of experimental animals. A number of studies have been conducted in which animals are exposed over periods of time to diluted LDMV exhaust gases using equipment functionally similar to the ARB/CVS sample bag systems (e.g., Pepelko et al. 1979, Pepelko 1981, Pepelko 1982). As noted earlier, given the high reactivity in vitro of HONO toward, for example, secondary amines (Hanst et al. 1977, Pitts et al. 1978, Tuazon et al. 1978), to yield highly carcinogenic nitrosamines, careful attention should be paid to the probable presence of elevated HONO levels in such exposure systems.

Our preliminary data do not allow for the elucidation of the mechanism(s) producing the observed HONO in sampled auto exhaust. However, current ARB supported research at these laboratories is designed to measure unambiguously the levels of HONO in LDMV exhaust freely emitted to the atmosphere.

Finally, it should be noted that our preliminary results were reported at the Symposium on "Biological Tests in the Evaluation of the Mutagenicity and Carcinogenicity of Air Pollutants with Special Reference to Motor Exhausts and Coal Combustion Products" at the Karolinska Institute in Sweden, and are now in press in Environmental Health Perspectives (Pitts 1982). Additionally, a paper discussing these initial studies is being submitted for publication in Environmental Science and Technology (Pitts et al. 1982).

II. DETAILED REPORT

A. Background

The critical role of hydroxyl (OH) radicals in the initiation of photochemical smog has been recognized for many years (see the review by Finlayson-Pitts and Pitts 1977, and the article on modeling by Carter et al. 1979). The main photolytic steps in the primary production of the chain-initiating OH radical involve aldehydes (especially formaldehyde), ozone and nitrous acid. Of these, ozone is generally not present prior to irradiation of real or simulated polluted atmospheres; hence it does not contribute significantly as a radical source to the production of oxidant in the early morning hours or during the first stages of chamber simulations. Few ambient air measurements of aldehydes have been made in the early morning hours, but aldehyde concentrations appear to be relatively low during that time of the day (Cleveland et al. 1977, Tuazon et al. 1980). Clearly then, determination of typical ambient concentrations of HONO is important to the understanding of the rates and mechanisms of the initiation of photochemical air pollution in urban air basins.

Nitrous acid has recently been detected and monitored in urban atmospheres by SAPRC researchers (Platt et al. 1980, Harris et al. 1982) using the longpath, differential optical absorption technique first described by Platt et al. (1979). Since June 1979 a series of measurements of nighttime ambient HONO levels at various sites in the South Coast Air Basin has been conducted by SAPRC researchers. In particular, the results of a study carried out during July and August of 1980 at California State University, Los Angeles (CSULA) raised interesting questions concerning the possible contribution of LDMV exhaust to the observed atmospheric burden of HONO. Table 1 gives the maximum predawn HONO concentrations measured in that study (and in studies at Riverside), as well as values of related parameters measured concurrently with the HONO maxima.

The ambient HONO maxima were highly variable. In general the values measured at Riverside were within the range 1-4 ppb, while the values observed at CSULA were considerably higher, particularly when Path II, which was shorter and closer to the roadway-level, was employed (see Figure 3). The highest pre-dawn HONO observed using this path was ~8 ppb,

Table 1. Maximum Concentrations of HONO and Related Parameters Detected in the Los Angeles Basin.

Date	Location	Time PST	[HONO] (ppb)	[NO_2] (ppb)	[NO] (ppb)	T[a] (^oK)	RH[a] (%)	β_{scat}[b]	[HONO]$_{eq}$[c] (ppb)	$\frac{[HONO]}{[HONO]_{eq}}$
5 Jul 80	Riverside	5:00	2.9	22	~1	289	78	56	~1	~2.9
6 Jul 80	Riverside	5:00	2.1	25	~1	289	72	29	~1	~2.1
7 Jul 80	Riverside	6:00	1.4	57	~6	291	63		~2	~0.70
10 Jul 80	CSULA, Path I	3:00	2.4	65	nd[d]	292	45	nd	nd	nd
11 Jul 80	CSULA, Path I	3:00	2.1	87	nd	294	55	nd	nd	nd
12 Jul 80	CSULA, Path I	3:00	1.1	49	nd	291	65	nd	nd	nd
16 Jul 80	CSULA, Path I	3:00	4.2	94	~100	296	50	nd	16	~0.26
17 Jul 80	CSULA, Path I	3:00	1.4	44	40	292	66	8	7	0.20
18 Jul 80	CSULA, Path I	3:00	1.8	50	25	292	70	8	6	0.30
19 Jul 80	CSULA, Path I	5:30	1.2	40	~5	291	78	21	~3	~0.24
20 Jul 80	CSULA, Path I	2:00	nd	66	~6	290	73	27	~3	nd
21 Jul 80	CSULA, Path I	5:30	1.5	49	~5	290	78	30	~3	~0.50
22 Jul 80	CSULA, Path I	3:00	2.8	76	6	291	78	36	4	0.70
23 Jul 80	CSULA, Path I	3:00	3.6	66	35	293	71	12	8	0.45
24 Jul 80	CSULA, Path I	5:30	3.2	57	22	293	73	18	6	0.53
25 Jul 80	CSULA, Path I	3:00	2.6	70	15	293	71	16	6	0.43
26 Jul 80	CSULA, Path I	3:00	4.1	80	45	293	71	20	10	0.41
27 Jul 80	CSULA, Path I	3:00	4.2	57	44	292	76	22	9	0.47
28 Jul 80	CSULA, Path I	3:00	4.4	83	44	294	66	14	10	0.44
29 Jul 80	CSULA, Path II	6:00	6.0	80	100	295	64	16	15	0.40
1 Aug 80	CSULA, Path II	5:30	7.5	120	90	298	54	17	16	0.47
5 Aug 80	CSULA, Path II	4:30	0.4	28	0	295	69	15	nd	nd
6 Aug 80	CSULA, Path II	4:00	3.6	57	12	292	78	14	5	0.72
7 Aug 80	CSULA, Path II	5:30	7.0	65	58	293	73	19	11	0.64
8 Aug 80	CSULA, Path II	6:00	8.0	105	100	295	57	20	16	0.50

[a]Given for 0600 PST.
[b]Relative units.
[c]Calculated equilibrium value for reaction $NO + NO_2 + H_2O \rightleftarrows 2\ HONO$.
[d]Not determined.

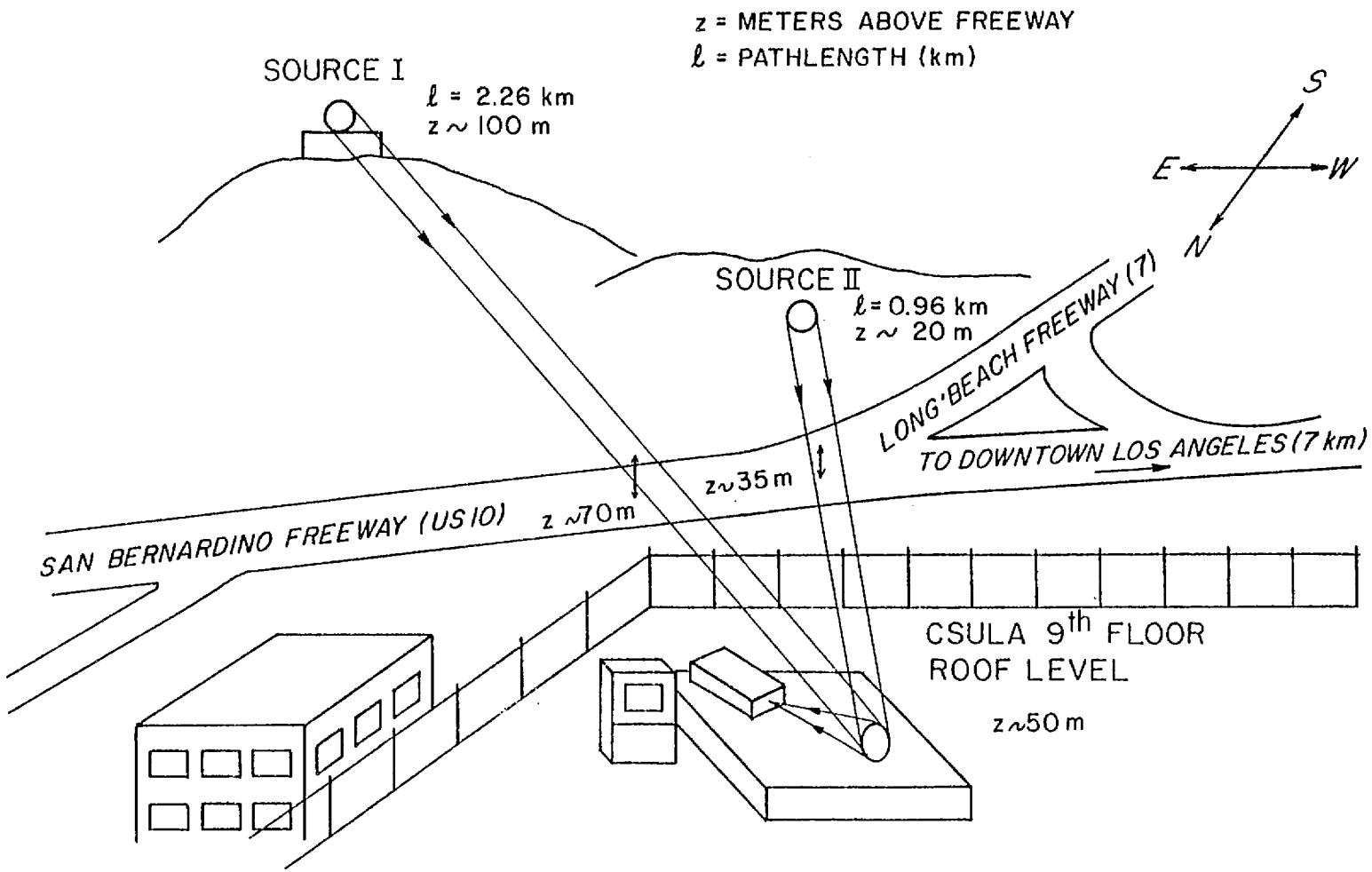

Figure 3. Diagram of the California State University, Los Angeles (CSULA) ambient air monitoring site used in measurements of atmospheric nitrous acid.

compared with 4.5 ppb observed using Path I, and 4 ppb previously observed at Riverside (Platt et al. 1980).

Representative morning concentration-time profiles for HONO and NO_2 in Riverside, and at CSULA using Path II, are shown in Figures 4 and 5, respectively. Generally, the nighttime concentration profile of HONO in Riverside tended to follow that of NO_2, with temporary HONO minima and maxima occurring at the same time as NO_2 minima and maxima (Figure 4). This suggests that most of the HONO had been previously formed and was being transported with NO_2 (and other pollutants) to Riverside. On the other hand, the HONO levels at CSULA increased steadily throughout the night, with no close correspondence in concentration-time profile with that of NO_2 (Figure 5). This suggests that HONO is either formed or emitted at that site rather than being transported from another location.

The mechanism for the observed nighttime increase in HONO concentration is still uncertain. The HONO levels observed at CSULA using Path II, with a larger relative contribution from the air mass directly over the freeway (Figure 3), were generally higher than those observed using Path I. This suggests the presence of higher HONO levels very near the freeway, which could be caused either by direct emission of HONO by LDMV or by its rapid formation from NO_x emitted by LDMV (before significant dilution occurred).

In considering the possible mechanisms for in situ formation of HONO (as opposed to direct emission), no simple formation mechanism accounts well for these observations. Possible formation mechanisms are:

$$OH + NO \xrightarrow{M} HONO \qquad (2)$$

$$NO + NO_2 + H_2O \rightleftarrows 2\ HONO \quad \text{(heterogeneous)} \qquad (3,-3)$$

$$2\ NO_2 + H_2O \rightarrow HONO + HONO_2 \quad \text{(heterogeneous)} \qquad (4)$$

Other reactions have been considered, but can be shown to be of negligible importance (Perner and Platt 1979).

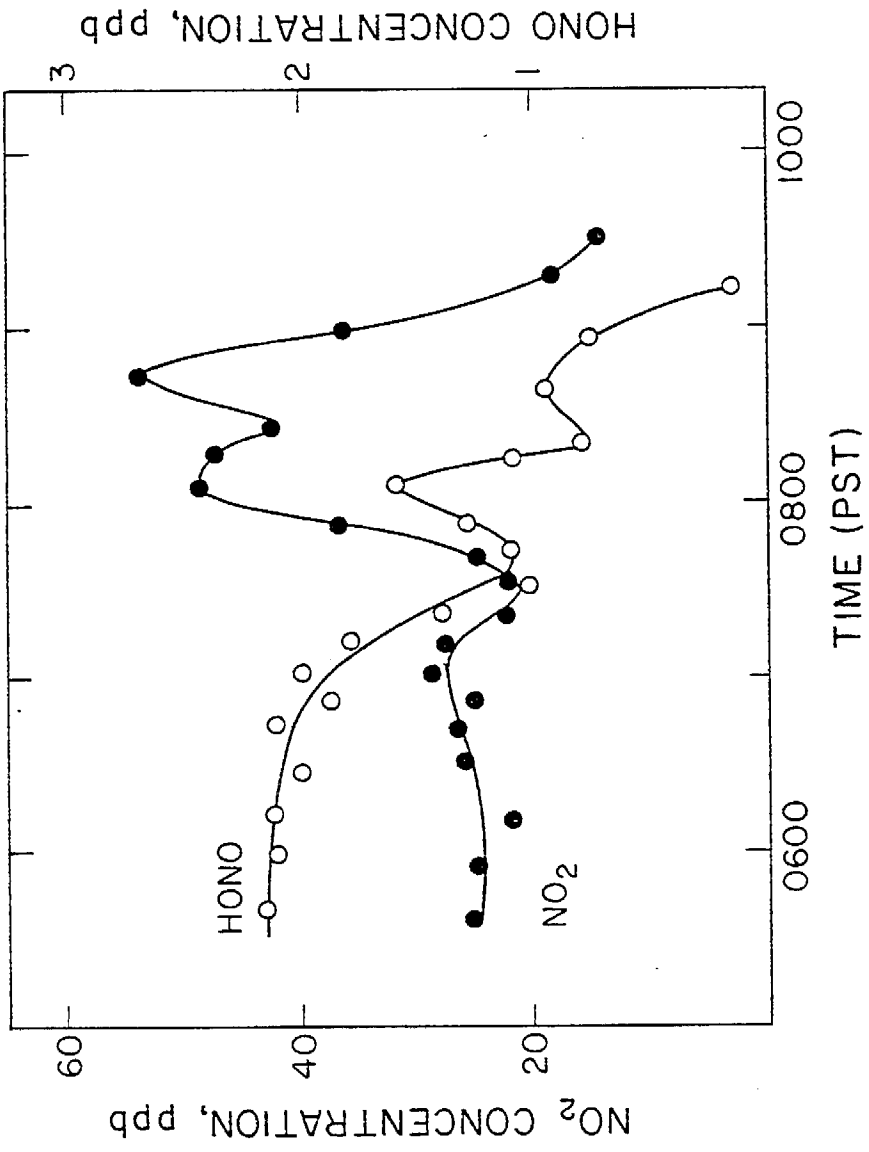

Figure 4. Concentration-time profiles for HONO (O) and NO_2 (●) measured by DOAS at Riverside, CA, July 6, 1980.

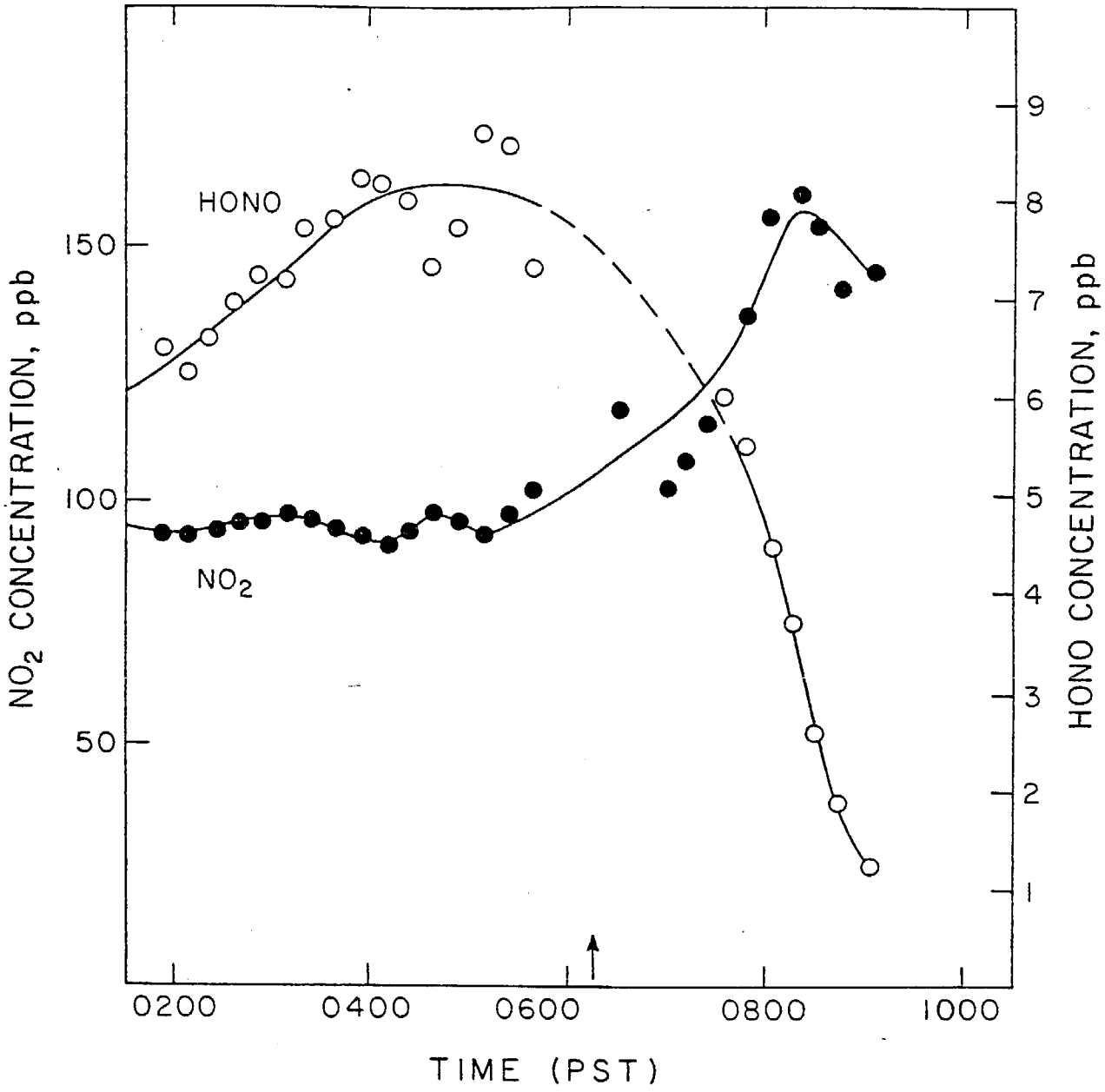

Figure 5. Concentration-time profiles for HONO (O) and NO_2 (●) measured by DOAS at CSULA, August 8, 1980.

If reaction (2) is the nighttime source of HONO, then the OH radicals must be formed from some nonphotolytic source. One possible dark source of OH radicals is the reaction of PAN [$CH_3C(O)OONO_2$] with NO. This could occur when NO is emitted into an air mass containing PAN, which has been formed photochemically on the previous day. Subsequent reactions involving NO and O_2 are known to result in the formation of OH radicals (Hendry and Kenley 1977, 1979, Carter et al. 1981). Unfortunately, available data are not sufficient to assess the importance of this reaction system on the days measurements were taken.

If reaction (3) is the source of HONO, it must proceed heterogeneously since (3) has been shown to be slow in the gas phase (Chan et al. 1976, Kaiser and Wu 1977). The possible role of reaction (3) as a source of HONO can be examined by comparing the observed HONO maxima with equilibrium values calculated on the basis of the known equilibrium constant (Chan et al. 1976) for reactions (3,-3) and measurements of NO_x and relative humidity (Table 1). It can be seen from Table 1 that at the CSULA site the observed HONO levels were 25-70% of the equilibrium concentrations, while at Riverside they exceeded the calculated equilibrium levels.

There is no simple correlation between $[HONO]/[HONO]_{eq}$ and aerosol levels as measured by nephelometry. Thus, the main formation mechanism cannot be described as a simple, aerosol surface-catalyzed approach to the $NO/NO_2/H_2O/HONO$ equilibrium. However, the rate of approach to equilibrium and the distribution of HONO between the gas and aerosol phases may in general be a complex function of aerosol size distribution, composition (especially pH), temperature, and relative humidity; it may thus be unreasonable to expect simple overall correlations and numerical relationships to hold.

The possibility of NO_2 hydrolysis [reaction (4)] as a contribution to HONO formation is suggested by the fact that HONO build-up was observed on several occasions in the evening at Riverside when NO concentrations were strongly suppressed by ozone. If reaction (4) is important, the nitric acid co-product will in part determine the pH of the droplet and in turn affect the distribution of HONO, formed in both reactions (3) and (4), between the solution phase neutral and ionic species, and the gas phase

molecular species. However, reported studies on the rate of reaction (4) in pure water (Ottolenghi and Rabani 1968, Sada et al. 1979, Komiyama and Inoue 1980, Lee and Schwarz 1981) indicate that the process is much too slow to explain the observed HONO formation. Even under favorable assumptions (10^{-2} g m^{-3} liquid water and equilibrium distribution of NO_2 between phases) application of rate data in the literature leads to predicted HONO formation rates about 4 orders of magnitude lower than those observed.

Thus while the formation chemistry for nitrous acid in polluted urban atmospheres is unclear, there remains strong circumstantial evidence that the significant amounts of the observed HONO may result from LDMV emissions. Either it is directly emitted with NO_x from LDMV exhaust, or it is formed from the emitted NO_x almost immediately after emission and then "frozen" by cooling and dilution. When describing the integrated source strength for HONO from LDMV in, for example, the South Coast Air Basin, it may make little difference which of these alternatives (<u>if either</u>) is the case. On the other hand, from the point of view of health effects implications for emission control technology, these alternatives are quite different.

B. Methods of Procedure

1. Optical System

The basic DOAS optical system, shown in Figure 1 (page 9) along with the other components of the DOAS spectrometer, is designed to project a collimated beam of light along an optical path whose length is chosen according to the required sensitivity for the particular experiment. The system consists of two principal parts: a light source and a light collector/detector unit.

(a) The light source is designed to emit a parallel beam of light free of spectral structure in the wavelength ranges of interest (i.e., emitting a continuum). This is accomplished by either using Xenon (Xe) high-pressure lamps (Osram XBO 450, Illumination Industries X-75) or incandescent lamps (150-240 W quartz-iodine), in combination with a "search light"-type focussing mirror.

(b) At the receiving end the transmitted light is collected by a Newtonian telescope and focussed on the entrance slit of a spectrograph. The spectrograph used in this work was a McPherson 0.3 m unit equipped with a 600 lines per mm grating.

2. Flow Cell and Exhaust Sampling

The first shortpath DOAS system designed for exhaust measurements under this contract utilized a sample cell constructed from a 1.5 m long, 7.6 cm diameter, borosilicate tube and fitted with quartz end windows mounted against Viton O-rings. The exhaust sample was directed to the apparatus through ID flexible metal tubing with a diameter of 5.1 cm and admitted to the cell through side arms with a diameter of 3 cm.

Preliminary experiments with this cell revealed several problems. The relatively narrow diameter of the inlet and outlet sidearms acted as a bottleneck to the rapidly flowing exhaust stream, and the resulting overpressuring in the feed pipes caused leakage of exhaust gas to the atmosphere. Moreover, it was feared that in prolonged runs this back pressure could lead to vehicle damage. Further experimental difficulty was associated with particulate deposition on the cell windows. These had to be frequently removed for cleaning, which lead to disruption of the testing schedule.

To overcome these difficulties, a second cell was designed and constructed. This was constructed from 10.2 cm-diameter polypropylene tubing and was fitted with 7.6 cm-diameter side arms. The side arms were angled at $\sim 60^{\circ}$ with respect to the long axis of the cell so that the windows, especially the one at the entrance end of the cell, were substantially protected from the direct exhaust gas flow. This resulted in much longer testing periods between required cleanings. Moreover, the mountings for the windows were redesigned to facilitate cleaning when necessary. Exhaust gases were directed to the cell through 10.2 cm diameter asbestos-lined, flexible metal tubing. With this new system no overpressuring was observed.

The overall optical path in this cell was 3.57 m, which resulted in an increase in sensitivity over the original cell of more than a factor of two. The final cell length was selected to optimize space utilization in the chassis dynamometer bay.

3. The Rapid Scanning Device

A 6 to 40 nm segment of the dispersed spectrum produced in the exit focal plane of the spectrograph is scanned by a series of moving exit slits etched radially in a thin metal disk (slotted disk) rotating in the focal plane. At a given time, one particular slit on the disk is used as an exit slit. The light passing through the exit slit is received by a photomultiplier tube, and the output signal is digitized by a high-speed analog-to-digital converter and read by a minicomputer. During one scan (i.e., one sweep of an exit slit over the spectral interval of interest), several hundred digitized signal samples are taken. Consecutive scans are performed at a rate of approximately 100 scans per second and are signal-averaged by the software.

The process of taking one spectral scan is illustrated in Figure 6. The central wavelength of the scan is selected by the spectrograph setting and the width of the scan region is controlled by a mask located very close to the slotted disk. The distance between the slits along the rim of the disk is slightly larger than the aperture of the mask, so that at any time no more than one slit is irradiated. As a slit becomes visible at the left edge of the mask, it is detected by an infrared light barrier located there (see Figure 6), and a trigger signal is sent to the computer. While the slit then sweeps over the spectrum, the computer continuously takes digitized samples of the light intensity at the current position of the slit. Thus, one sweep of a slit is divided into several hundred channels, each associated with a wavelength interval several times narrower than the resolution for the spectrograph. During each scan, the digitized samples are added to the corresponding channels in the computer memory, and all consecutive scans are superimposed in the computer memory (signal averaged).

After one scan is complete, the next trigger pulse will indicate to the computer that the next slit (shown in dashed lines in Figure 6) is approaching the left edge of the mask. In order to preserve the spectral resolution while superimposing a large number of individual scans, the rotational speed of the slotted disk is kept constant to within ± 0.5%.

Signal variations detected by the computer during a single spectral scan can be caused by several effects:

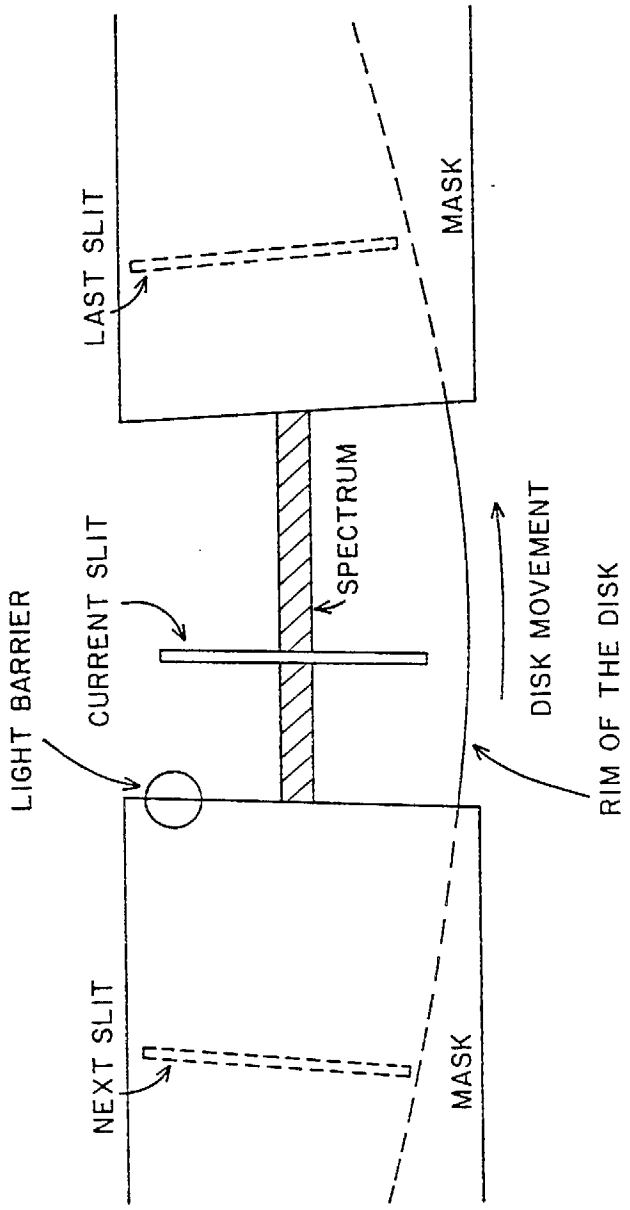

Figure 6. "Slotted disc" rapid scanning device located in the exit focal plane of the spectrograph.

(1) The light absorption by trace gases may vary with wavelength.

(2) The light losses due to mirror reflectivities, etc., may vary with wavelength.

(3) The output of the light source may vary with wavelength and time.

(4) Optical refraction may change with time (e.g., due to turbulence in the exhaust flow).

(5) Random noise is added to the signal by the photomultiplier, preamplifier and A/D converter.

Since a single spectral scan takes only ~10 msec, the effect of turbulence in the exhaust gas flow is very small. Moreover, typical spectra obtained during several minutes of integration time represent an average of over 10,000-40,000 individual scans. Thus, effects of noise and temporal signal variations are very effectively averaged. In fact, even entire, momentary blocking of the light beam has no noticeable effect in the spectrum.

4. Processing of Absorption Spectra

The raw spectra will usually show an overall slant due to the spectral distribution of the light source and the reflection (or transmission) characteristics of the optical components (grating and mirrors). In order to remove this overall feature, the spectrum is divided by a fitted polynomial of first to fifth order. The "narrow" features (extending only over a narrow wavelength range) caused by trace gas absorption are not significantly affected by the process.

The trace gas concentration c is derived from the spectrum by applying Beer's law:

$$c = (\log I_o/I)/(\varepsilon \ell) \qquad (5)$$

where I_o = incident light intensity without absorption by the trace gas

I = transmitted light intensity, reduced because of absorption by the trace gas

$\log (I_o/I)$ = optical density (OD)

ε = differential absorption coefficient of the trace gas

ℓ = length of the light path

Since the true incident light intensity (I_o) cannot be obtained with this method, the "differential" optical density is used to evaluate the trace gas concentration (see Figure 7). The differential optical density is defined by log I_o'/I where I_o' is the intensity (at wavelength λ_2) in the absence of the particular absorption structure, rather than in the absence of any absorption at all (as indicated by the dashed line labeled "True" I_o in Figure 7). According to this definition, I_o' can be calculated from $I(\lambda_1)$ and $I(\lambda_3)$:

$$I_o' = I(\lambda_1) + [I(\lambda_3)-I(\lambda_1)] \cdot \frac{\lambda_2-\lambda_1}{\lambda_3-\lambda_1} \qquad (6)$$

Of course, the absorption coefficient ε has to reflect the above definition of I_o'; accordingly the "differential absorption coefficient" of a trace gas will generally be lower than its conventional "total absorption coefficient" at the same wavelength.

In the practical application of the DOAS instrument, the precision of the measurements is improved by least squares fitting of a reference spectrum of the substance under consideration to the observed absorption spectrum. Thus, all absorption bands of a given substance in the scanned spectral region, as well as the information contained in their relative strengths and particular shapes (the "fingerprint" of the substance), are used. This method even allows the deconvolution of overlapping spectra of different species to obtain the concentration of the contributing components with good accuracy.

5. Software

The in-house software for the DOAS spectrometer performs three major tasks (Figure 8):

(1) Individual spectral scans are signal-averaged in the computer memory and displayed on an oscilloscope screen.

(2) System "housekeeping" (e.g., monitoring signal intensity, counting of scans, etc.) is carried out as a "background" task.

(3) Application of a large number of mathematical functions to the acquired absorption spectra is carried out to extract the trace gas concentrations from the observed spectra. Also, spectra can be stored and recalled on mass storage devices (e.g., disks).

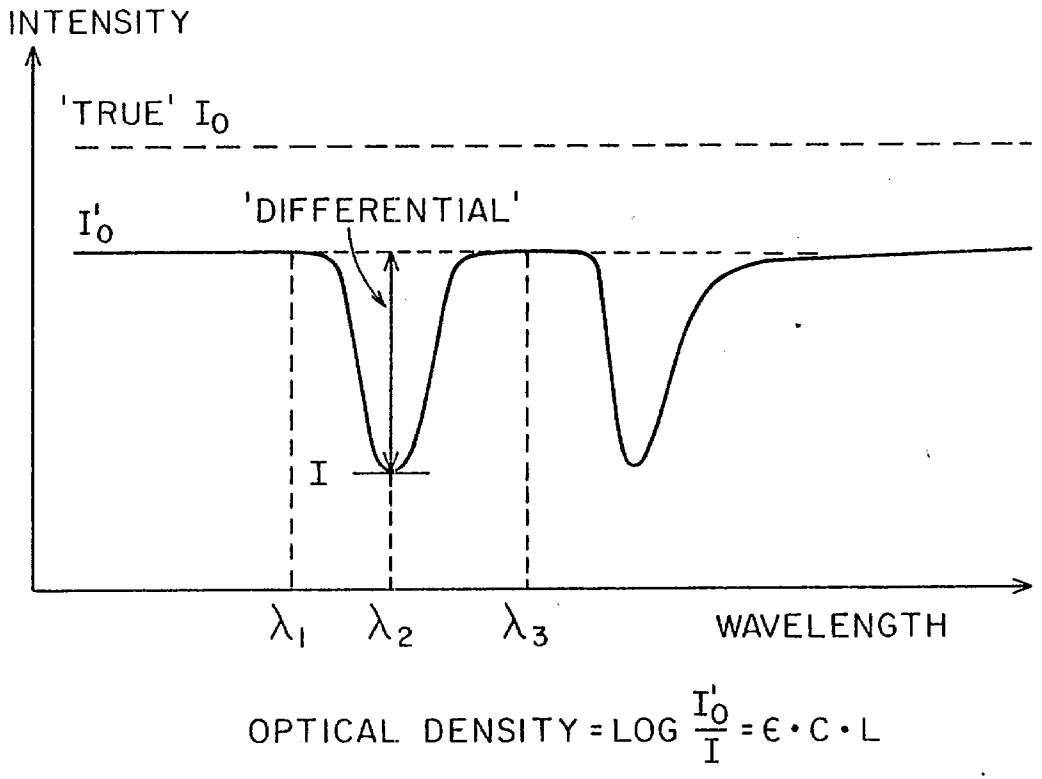

Figure 7. Representation of the definition of the term "differential optical density," where ϵ = the "differential absorption coefficient."

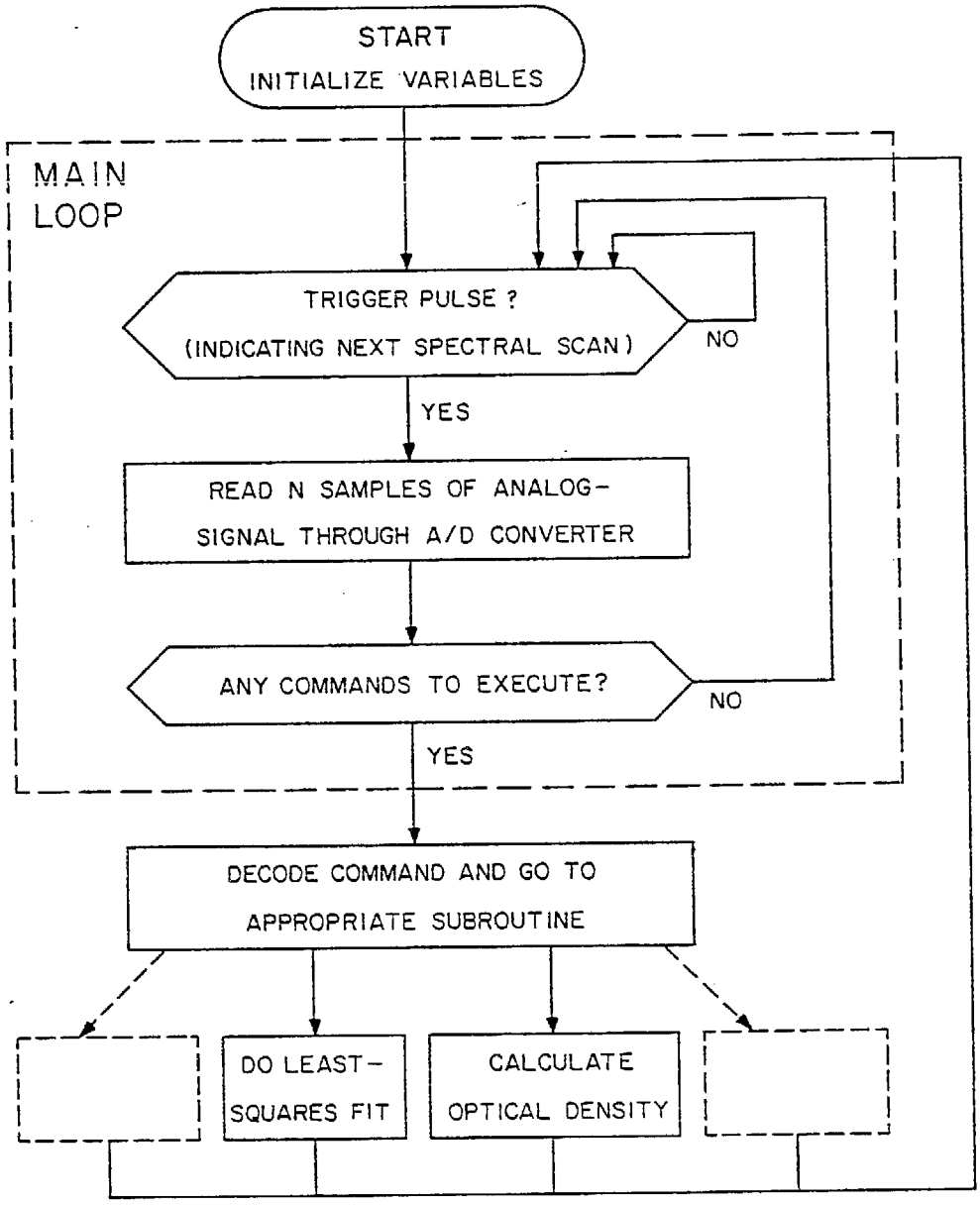

Figure 8. Software flow chart for the DOAS system.

The program is written in MACRO 11 and FORTRAN IV for use with Digital Equipment PDP 11 computers.

The mathematical functions available for manipulation of the absorption spectra include multiplication and division by a constant factor, addition and subtraction of two spectra, division by a least squares fitted polynomial, shifting of the spectra in wavelength, change of the wavelength scale ("expansion" and "compression" of a spectrum), calculation of the differential optical density of an indicated absorption band, least squares fitting of up to four reference spectra to a given spectrum, and calculations of the logarithm of a spectrum. In addition to these, several hardware functions, including those to change the wavelength setting of the spectrometer or to move a filter into the light path, are controlled by the software. All software functions can be executed in automatic sequences.

6. Detection Limits of the DOAS System

The detection limit for a particular substance can be calculated according to equation (5) if the differential absorption coefficient, the minimum detectable optical density (OD) and the length of the light path are known. While, for a given minimum detectable OD, the detection limit theoretically improves proportionally to the length of the light path, this does not mean that in practice the actual detection limit always improves with a longer light path. With a longer light path the received light intensity $I(\lambda)$ tends to be lower; this increases the noise associated with the measurements of $I(\lambda)$ and thus increases the minimum detectable OD. In addition, the minimum detectable OD will be higher if it is necessary to subtract overlapping absorption features of other species (see below). With a typical DOAS system (using a Xe light source), minimum detectable optical densities of $1\text{-}2 \times 10^{-4}$ (base 10) can be achieved for several minutes of averaging time at wavelengths $\geq$ 300 nm.

7. Measurement Protocols

An original goal of this program was to perform measurements on whole exhaust by feeding emissions from the tailpipes of a series of LDMV directly to the sample cell. The exploratory experiments with the original 1.5 m cell were so conducted. However, the loss of the evening work shift at the ARB Haagen-Smit Laboratory restricted the use of the

dynamometer bays to ARB activities other than our experiments using the longer, improved sample cell. Moreover, concern by the ARB staff that insertion of the optical cell between the vehicle tailpipe and the CVS system might inadvertently modify ARB data made it impractical to "piggy-back" on dynamometer runs being performed for other purposes.

Thus, the experimental procedure was modified to perform most of the monitoring experiments on the effluent from the ARB CVS system (point C, Figure 2, page 11). This arrangement had some disadvantages for the interpretation of data (especially on HONO levels) since the raw exhaust gases from the tailpipe were exposed to large areas of metal and other surfaces, and were diluted by ambient air (at ambient temperatures). However, use of the CVS system allowed spectroscopic measurements to be made during dynamometer runs performed under other ARB programs without undue inconvenience to ARB personnel. The bulk of our DOAS measurements were thus made on vehicles being tested concurrently by the ARB for various other programs. Spectroscopic analyses of the contents of a small number of sample bags filled (at point B, Figure 2) according to standard ARB practice were also performed, and the results compared with those of routine ARB methodologies.

Measurements were made for three test protocols: the Cold CVS II Test, the Loaded Mode Test and the Highway Driving Cycle. The Cold CVS II Test consists of three phases: (I) a "cold" (~70°F) engine start initiating an ~8 min sample collection; (II) a further sample collection during a 14-minute cruise (which is followed by a 10-minute engine-off period); and (III) a warm start and eight-minute cruise sample. The Loaded Mode test also consists of three phases: a high-speed loaded cruise, a low speed loaded cruise and an engine idling phase. The Highway Driving Cycle test is designed to provide a standard "gm per mile" emission figure.

C. Results

The range of vehicles studied included model years from 1973 to 1981 having a wide variety of engine displacements and emission control devices. The amounts of HONO and NO_2 observed (and the ratio of these quantities) appeared to vary as much between similar vehicles as between vehicles with different engine sizes, emission control equipment, etc.

Therefore the measurements are classified by operating mode rather than by vehicle type.

1. Highway Driving Cycle Test

Results for twelve similar tests conducted on a variety of vehicles are given in Table 2. The spectra for these tests were obtained from the contents of the 3.57 m flow cell through which the diluted auto exhaust effluent from the CVS system was passed (point C, Figure 2, page 11). Reference spectra of NO_2, HCHO and HONO are shown in Figure 9.

Figure 10 shows the spectra from a 1977 Mercury Bobcat station wagon (engine displacement 171 in^3, standard control equipment, odometer reading 23,939 miles). The uppermost trace shows the complete spectrum in the ~40 nm spectral region centered on 355 nm after the cell background and the overall curvature of the spectrum were removed (as described above). The middle trace is a reference spectrum of NO_2. It can be seen that most of the spectral features in the exhaust spectrum arise from NO_2. However, close inspection of the relative intensity in the "doublet" of absorption bands near the center of the spectrum reveals that an additional absorber is present in the exhaust gas stream and that this absorber is intensifying the left hand member of this pair of bands.

The lowest trace in Figure 10 shows the result of dividing the exhaust spectrum by a computer scaled NO_2 reference, as described earlier (the normalized result has been multiplied by four for clarity of display in this figure). The resulting spectrum clearly shows three absorption bands at 342, 354 and 368 nm; these are due to nitrous acid. Application of Beers Law and the known absorption coefficients for these bands (Perner and Platt 1979) and for those due to NO_2 leads to the result that mean concentrations of 18.0 ppm NO_2 and 0.74 ppm HONO were present in DOAS sample cell during this test. This NO_2 level falls near the top end of the range of values observed for the twelve vehicles (Table 2) and, because of spectral overlap between NO_2 and HCHO (mentioned above), the formaldehyde concentration in the flow tube could not be quantified for this test.

Table 2. Data from DOAS Measurements of Diluted LDMV Exhaust: Standard Highway Driving Cycle Operating Mode

Vehicle	Year	Disp/Cyl/Trans[a]	ARB Test Code	Catalyst-Equipped	Odometer (miles)	NO_2 (ppm)	HONO (ppm)	HONO / NO_2	HCHO (ppm)
Oldsmobile Cutlass	73	350/8/A3	2S80C1/271/1B	No	92,438	0.58	0.11	0.19	2.8
Ford F-100 Pickup	75	360/8/M4	2S80C/275/2C	Yes	89,063	0.33	--	--	2.3
Buick	77	403/8/A3	2S80C1/269/2C	Yes	71,277	0.15	0.04	0.27	0.6
Mercury Bobcat	77	171/4/A3	2S80C1/286/1B	Yes	23,939	18.0	0.74	0.04	nd[b]
Datsun 280ZX	79	102/6/M5[c]	2S80C1/276/2L	Yes	8,884	0.49	0.06	0.12	0.3
Ford Mustang	80	140/4/A3	2S80C1/285/1B	Yes[d]	12,112	1.49	--	--	nd
Ford Mustang Turbo	80	140/4/M4[e]	2S80C1/274/1B	Yes	13,509	11.3	0.58	0.05	
Ford F100 Custom Pickup	80	300/8/M4	2S80C1/287/1B 2S80C1/287/2C[f]	Yes	9,758	20.6 17.1	0.59 0.44	0.03 0.03	nd nd
Ford LTD	80	351/8/A4	2S80C1/288/1B	Yes[d]	25,911	1.31	--	--	nd
BMW 320i	80	108/4/M5[c]	2V8106/1/1B	Yes[d]	4,577	0.09	--	--	nd
Chevrolet Monte Carlo	80	305/8/A3	2V8103/1/4D	Yes[d]	7,136	0.49	0.06	0.12	nd
Chevrolet Corvette	81	350/8/A3	2V8104/1/1B[f]	Yes[d]	3,201	1.28	0.09	0.07	0.5

[a]Engine displacement (in^3)/number of cylinders/transmission type, A - Auto, M - Manual.
[b]Not determined.
[c]Fuel injection.
[d]Three-way catalyst.
[e]Turbo charged vehicle.
[f]49 States car.

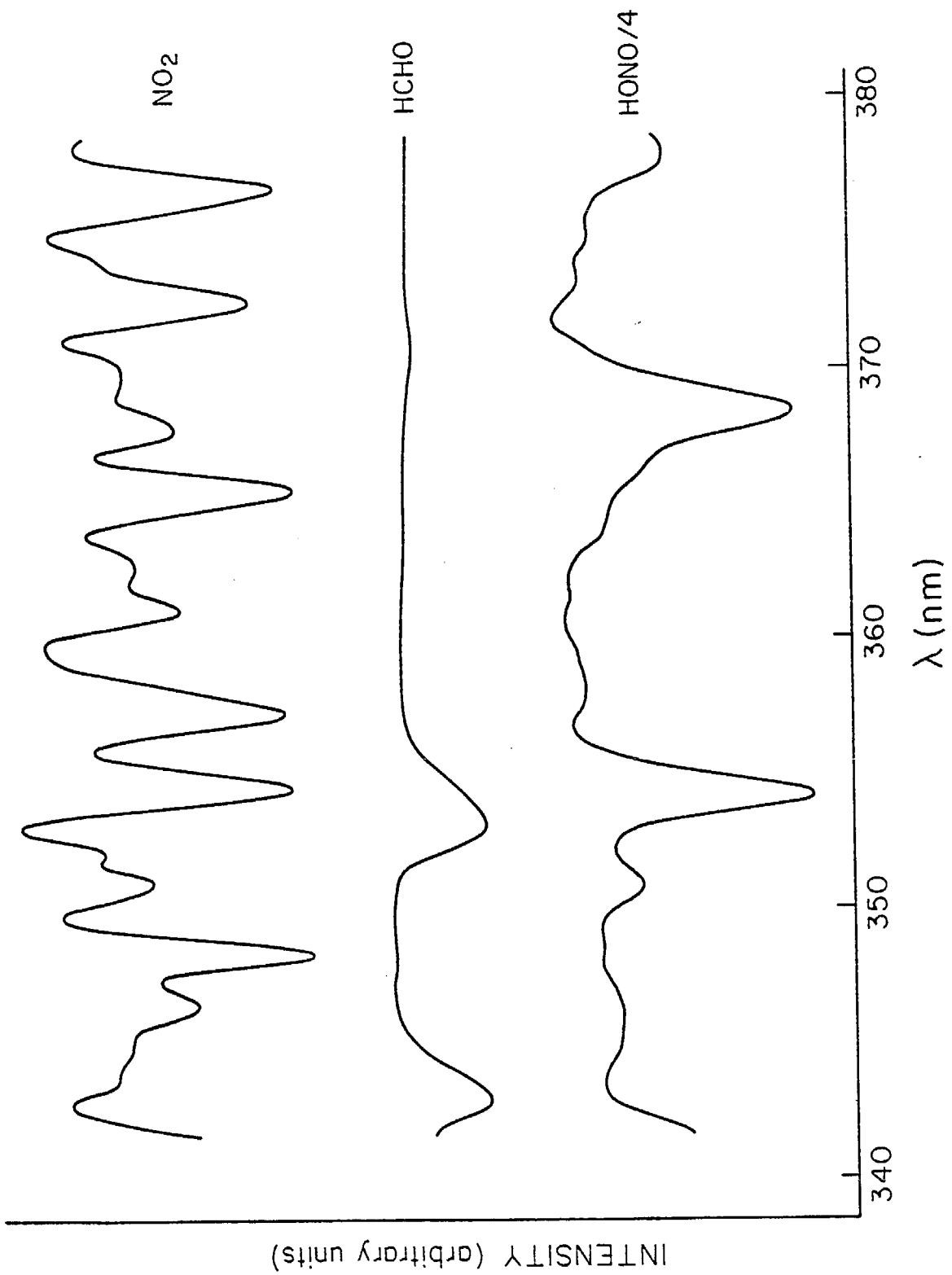

Figure 9. Reference spectra for nitrogen dioxide, formaldehyde and nitrous acid (scale of HONO spectrum reduced by a factor of 4).

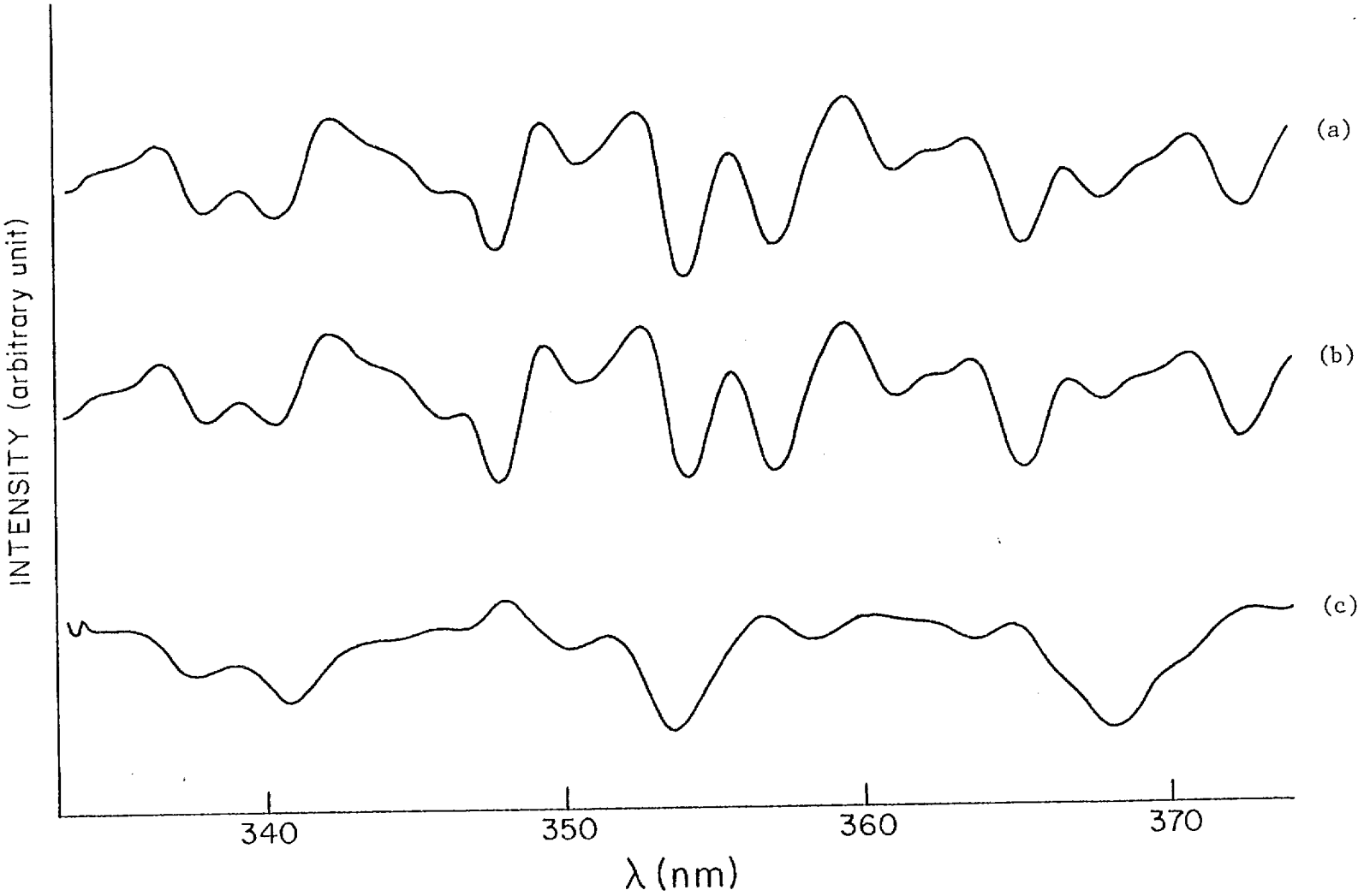

Figure 10. DOAS spectra acquired during a standard highway driving cycle test of a 1977 Mercury Bobcat. [a] Spectrum from the CVS system at point C in Figure 2 (page 11); [b] computer-fitted NO_2 spectrum (x4); [c] result of normalized division of (a) by (b) showing the three absorption bands due to HONO.

2. Cold CVS II Test Sequence

Results for six vehicles are summarized in Table 3. Spectra from a 1975 Ford pickup truck (engine displacement, 360 in^3, standard control equipment, odometer reading 89,063 miles) are shown in Figures 11-13.

Figure 11 shows the DOAS spectrum of diluted exhaust (uppermost trace, a) acquired during phase I of the test procedure [which includes a cold (~68°F) engine start with a 505 sec sample collection]. For illustrative purposes, our procedure for factoring out the contributions of NO_2 and HCHO to this exhaust sample spectrum (a in Figure 11) is shown step by step in Figure 11. The second trace (b) is the computer-fitted, NO_2 reference spectrum (multiplied by four), while the third trace (c) is the exhaust spectrum with features due to NO_2 removed. The fourth trace (d) is the computer-fitted formaldehyde spectrum, while the final trace (e) is the residual exhaust spectrum obtained following removal of both NO_2 and HCHO features. This clearly shows the three characteristic bands due to HONO. The concentrations of the three species in the flow tube during the first phase of this CVS II procedure were calculated from these spectra to be 0.78 ppm NO_2, 0.24 ppm HONO and 3.87 ppm HCHO.

Spectra acquired during phases II and III of the same CVS II test on this 1975 Ford pickup truck are shown in Figures 12 and 13, respectively. During phase II of the test (Figure 12) the dominant features of the exhaust spectrum (trace a) are again caused by formaldehyde. The second and third traces show the fitted NO_2 spectrum (multiplied by four) and the fitted HCHO spectrum; the lowest trace shows the residual spectrum, which again exhibits pronounced structure due to HONO. The calculated concentrations for this experiment are 0.24 ppm NO_2, 0.05 ppm HONO and 0.60 ppm HCHO. Although the signal-to-noise ratio is still large enough for positive identification of the three HONO bands (spectrum d), it is approaching unity, and therefore the detection limit is being reached.

Figure 13 shows spectra obtained during the third phase of the CVS II test on this vehicle. From these we calculate concentrations of 0.52 ppm NO_2, 0.13 ppm HONO and 2.70 ppm HCHO in the dilute exhaust gases.

3. Loaded Mode Test

Results for four vehicles are given in Table 4. Spectra acquired during the three phases of this test on a 1980 Ford F100 pickup truck

Table 3. Data from DOAS Measurements of Diluted LDMV Exhaust: Cold CVS II Operating Mode

Vehicle	Year	Disp/Cyl/Trans[a]	ARB Test Code	Catalyst (Y/N)	Odometer (miles)	Test Phase[b]	NO_2 (ppm)	HONO (ppm)	$\frac{HONO}{NO_2}$	HCHO (ppm)
Ford F-100 Pickup	75	360/8/M4	2S80C1/275/2C	Yes	89,063	I	0.78	0.24	0.31	3.9
						II	0.24	0.05	0.21	0.6
						III	0.52	0.13	0.25	2.7
Datsun 280ZX	79	102/6/M5[c]	2S80C1/276/2L	Yes	8,884	I	1.10	0.23	0.21	0.6
						II	0.41	0.07	0.17	0.5
						III	1.19	0.19	0.16	nd[d]
Datsun Pickup	80	120/4/M5	2S80C1/279/1B	Yes	24,654	I	0.46	0.11	0.24	1.8
						II	0.39	0.05	0.13	0.5
						III	1.13	0.14	0.12	1.5
Chevrolet Monte Carlo	80	305/8/A3	2V8103/1/4D	Yes[e]	7,136	I	1.39	0.25	0.18	2.3
						II	0.06	--	--	nd
						III	0.67	0.12	0.18	nd
Buick Skylark	80	173/6/A3	2S80C1/267/2L	Yes	15,222	I	1.16	0.50	0.43	nd
						II	0.26	0.05	0.19	nd
						III	1.22	0.19	0.16	nd
Chevrolet[f] Corvette	81	350/8/A3	2V8104/1/4B	Yes[e]	3,201	I	1.54	0.33	0.21	1.7
						II	2.15	0.15	0.07	nd
						III	1.60	0.15	0.09	nd

[a] Displacement (in^3)/No. of cylinders/transmission type, A - Auto, M - Manual.
[b] I - Cold start, 505 sec cruise (first ARB sample bag).
II - 862 sec cruise (second ARB sample bag).
III - 505 sec cruise following 10-minute soak period.
[c] Fuel injection.
[d] Not determined.
[e] Three-way catalyst.
[f] 49 States car.

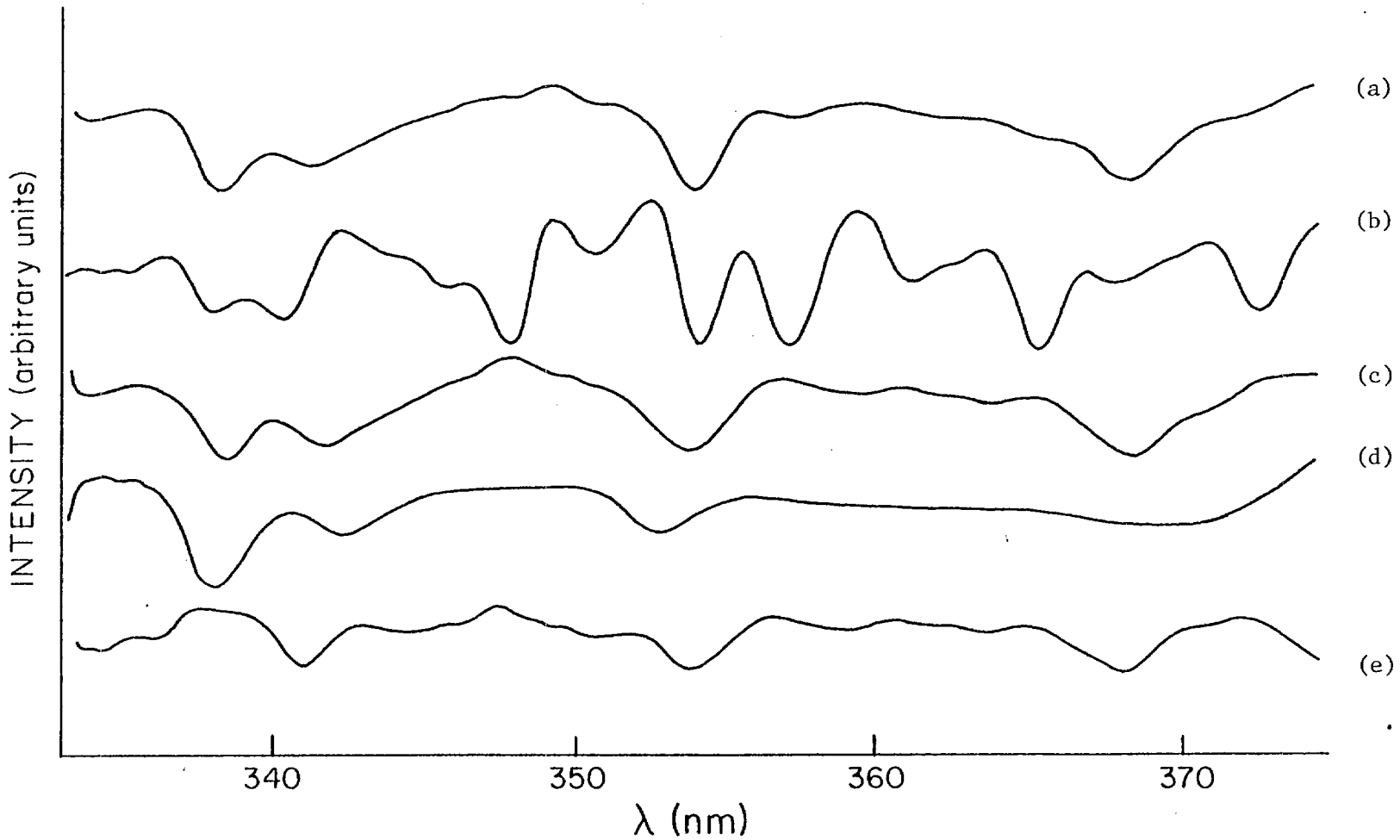

Figure 11. DOAS spectra acquired during phase I of a cold CVS-II test of a 1975 Ford pickup. [a] Spectrum from the CVS system at point C in Figure 2 (page 11); [b] computer-fitted NO_2 spectrum (x4); [c] result of normalized division of (a) by (b); [d] computer-fitted HCHO spectrum; and [e] result of normalized division of (c) by (d) showing the three absorption bands due to HONO.

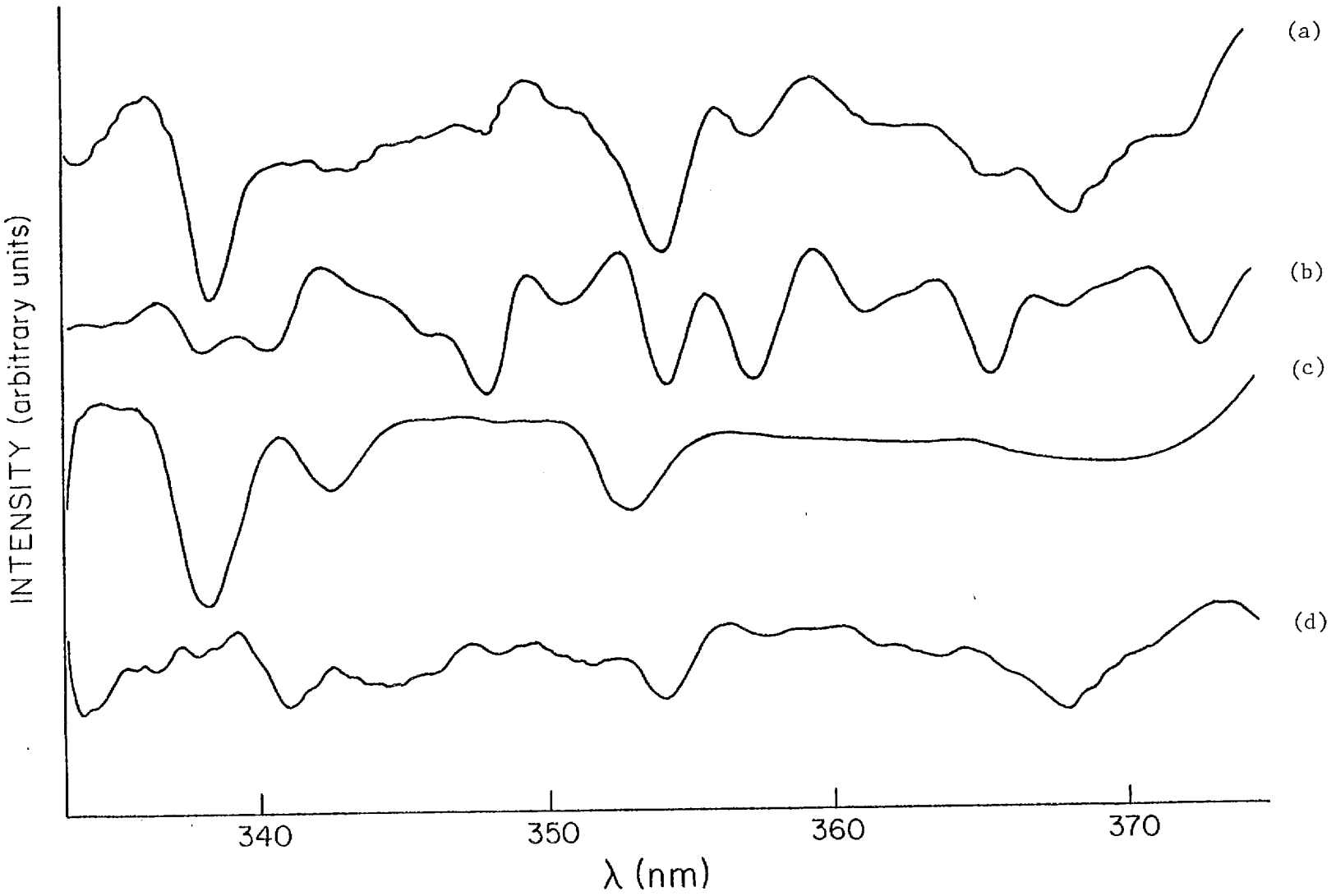

Figure 12. DOAS spectra acquired during phase II of a cold CVS-II test of a 1975 Ford pickup. [a] Spectrum from the CVS system at point C in Figure 2 (page 11); [b] computer-fitted NO_2 spectrum (x4); [c] computer-fitted HCHO spectrum; and [d] result of normalized division of (a) by (b) and (c) showing the three absorption bands due to HONO.

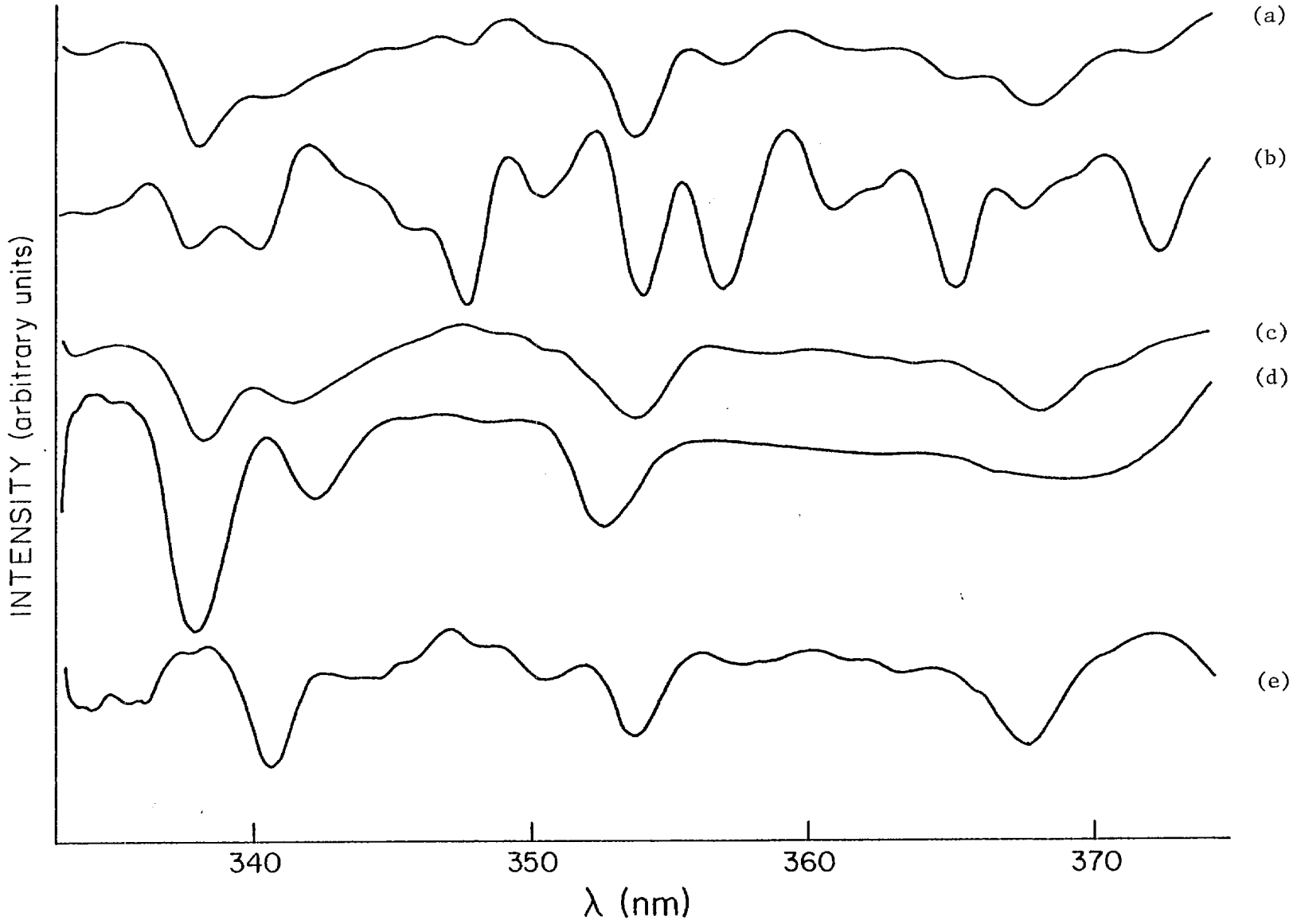

Figure 13. DOAS spectra acquired during phase III of a cold CVS-II test of a 1975 Ford pickup. [a] Spectrum from the CVS system at point C in Figure 2 (page 11); [b] computer-fitted NO_2 spectrum (x4); [c] result of normalized division of (a) by (b); [d] computer-fitted HCHO spectrum; and [e] result of normalized division of (c) by (d) showing three absorption bands due to HONO.

Table 4. Data from DOAS Measurements of Diluted LDMV Exhaust: Loaded Operating Mode

Vehicle	Year	Disp/Cyl/Trans[a]	ARB Test Code	Catalist (Y/N)	Odometer (miles)	Test Phase[b]	NO_2 (ppm)	HONO (ppm)	$\frac{HONO}{NO_2}$	HCHO (ppm)
Ford F100 Custom Pickup	80	300/6/M4	2S80C1/287/1B	Yes	8,781	HC	29.9	2.59	0.09	nd[c]
						LC	10.7	0.66	0.06	nd
						Idle	5.2	0.51	0.09	nd
Ford F100 Custom Pickup	80	300/6/M4	2S80C1/287/2C[d]	Yes	8,781	HC	26.7	1.40	0.05	nd
						LC	24.0	1.46	0.06	nd
						Idle	1.77	0.14	0.08	nd
Ford F100 Custom Pickup	80	300/6/M4	2S80C1/287/2C (no air)[e]	Yes	8,781	HC	9.92	1.27	0.13	nd
						LC	17.5	2.88	0.17	nd
						Idle	2.90	0.73	0.25	nd
Ford Mustang	80	140/4/A3	2S80C1/285/1B	Yes[f]	12,112	HC	2.32	0.66	0.28	nd
						LC	0.75	0.18	0.24	nd
						Idle	0.30	--	--	nd
Ford Mustang Turbo	80	140/4/M4	2S80C1/274/1B	Yes	13,509	HC	2.41	0.97	0.42	nd
						LC	15.3	1.94	0.13	nd
						Idle	1.42	0.78	0.55	nd
Ford F100 Pickup	75	360/8/M4	2S80C1/275/2C	Yes	89,063	HC	0.54	0.10	0.18	3.0
						LC	--	--	--	1.1
						Idle	--	--	--	1.9
Ford F100 Pickup	75	360/8/M4	2S80C1/275/2C (no air)[e]	Yes	89,063	HC	0.64	--	--	2.6
						LC	0.07	--	--	0.7
						Idle	--	--	--	2.1

[a]Displacement (in^3)/No. of cylinders/transmission type, A - Auto, M - Manual.
[b]Test phase: HC - high speed loaded cruise, LC - low speed loaded cruise, Idle.
[c]Not determined.
[d]Same test procedure after tuneup.
[e]Mechanism for pumping air to exhaust manifold disabled.
[f]Three-way catalyst.

(engine displacement, 300 in^3, standard control equipment, odometer reading 8,781 miles) are shown in Figures 14 to 16. When operating under high load this vehicle produced the highest levels of NO_2 (29.9 ppm) and HONO (2.59 ppm) observed in any vehicle run on any of the tests in the flow tube mode. Because of the high NO_2 level the contribution of formaldehyde to the DOAS spectrum was obscured and no HCHO data could be obtained.

4. Nitrous Acid Measurements of Dilute Exhaust Collected in a Sample Bag

A sample bag was filled (at point B, Figure 2) with a mixture of air and exhaust gases in one experiment (dilution factor of 5.12) from a 1980, six-cylinder, 300 in^3 Ford pickup (mileage = 2,381) run on a Standard ARB Highway Cycle. This pickup was already known to have high NO_x emissions. Within 1-2 minutes after filling, the contents of the bag were flushed through the DOAS cell and the concentrations of HONO and NO_2 determined. Results are shown in Table 5. An ARB chemiluminescence analysis of the same sample gave $[NO_2]$ (= [total NO_x - NO]) = 69 ppm, which is in good agreement with the DOAS value for $[NO_2]$ of 67 ppm. The 8.5 ppm of HONO comprised ~4% of the NO_x in the bag and was present at ~13% of the NO_2 concentration.

Table 5. Concentrations of HONO and NO_2 Determined by the DOAS System, and NO_x and NO by the ARB Chemiluminescence Method, in a Sample Bag Filled at Point B (Figure 2) for a 1980 Ford Pickup (Six-Cylinder, 300 in^3 Engine) Operated at Standard ARB Highway Driving Cycle

DOAS Analysis of Sample Bag Contents[a]	
HONO	8.5 ppm
NO_2	67 ppm
$HONO/NO_2$ = 0.13	
ARB Chemiluminescence Analysis of Sample Bag Contents	
Total NO_x	210 ppm
NO	141 ppm
$[NO_x-NO] = NO_2$	69 ppm
$HONO/NO_x$ = 0.04	

[a]Bag dilution factor: 5.12; T = 24.4°C, RH = 48.2%.

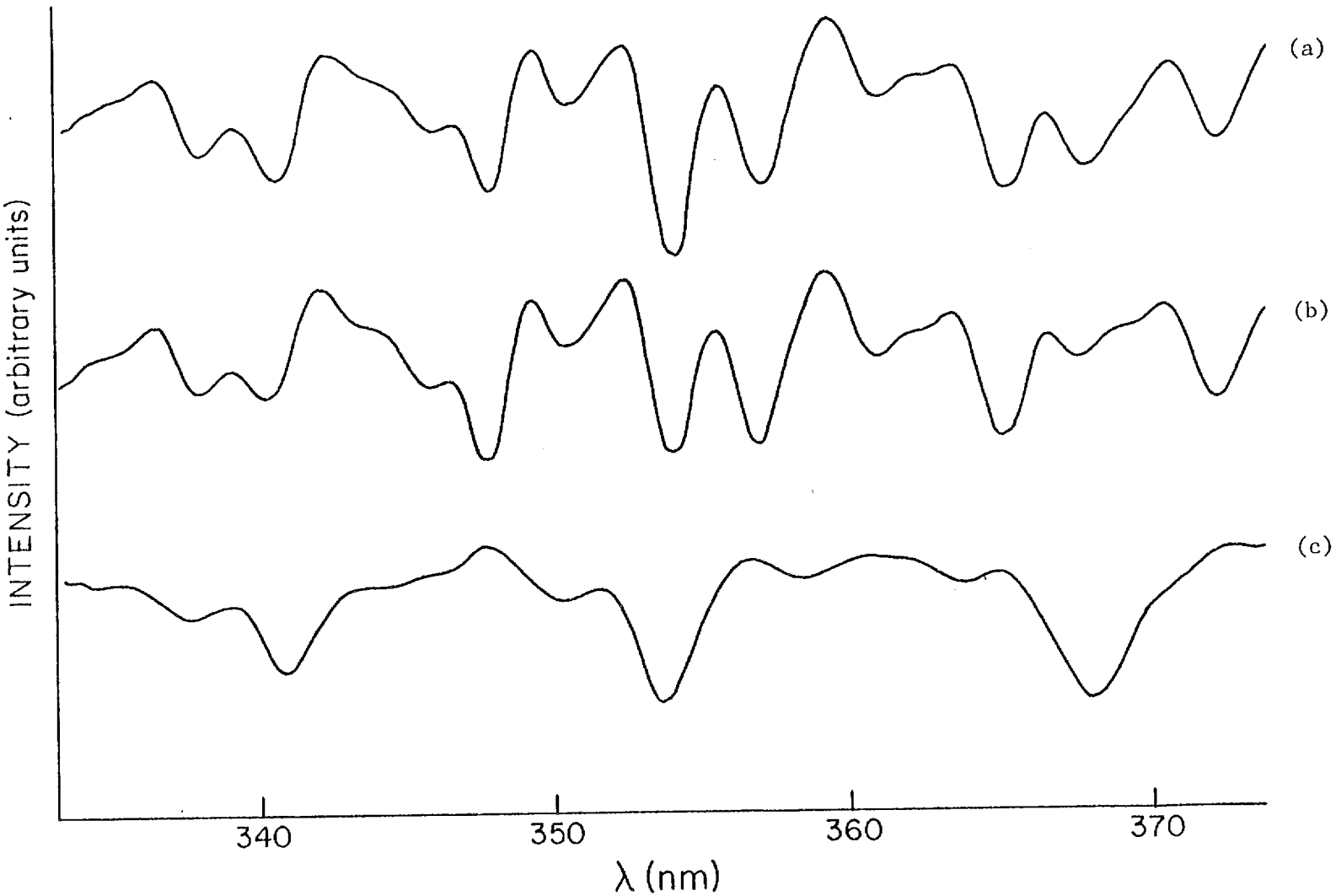

Figure 14. DOAS spectra acquired during phase I (high cruise) of a loaded mode test of a 1980 Ford F-100 pickup. [a] Spectrum from the CVS system at point C in Figure 2 (page 11); [b] computer-fitted NO_2 spectrum (x4); [c] result of normalized division of (a) by (b) showing features due to HONO.

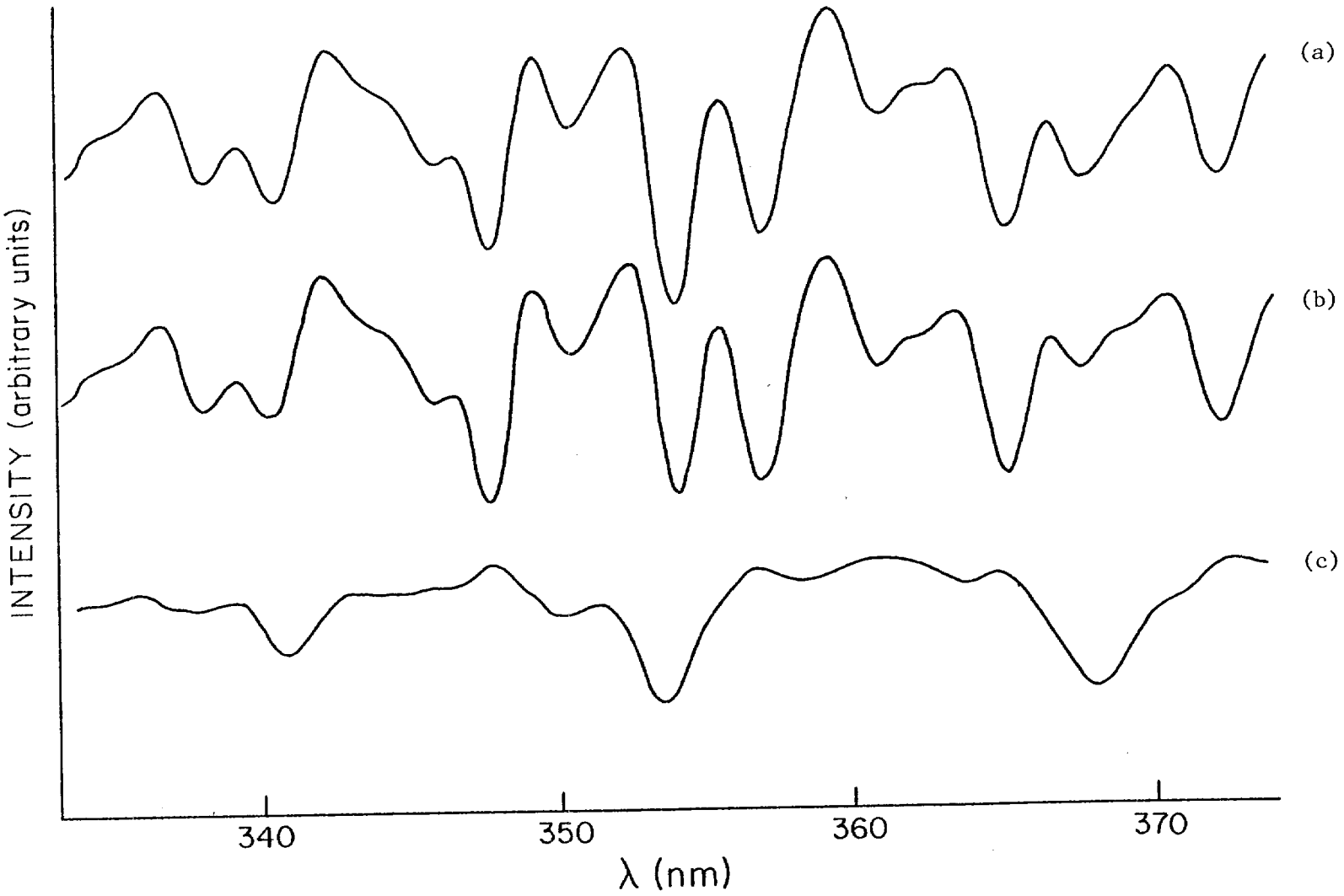

Figure 15. DOAS spectra acquired during phase II (low cruise) of a loaded mode test of a 1980 Ford F-100 pickup. [a] Spectrum from the CVS system at point C in Figure 2 (page 11); [b] computer-fitted NO_2 spectrum (x4); [c] result of normalized division of (a) by (b) showing features due to HONO.

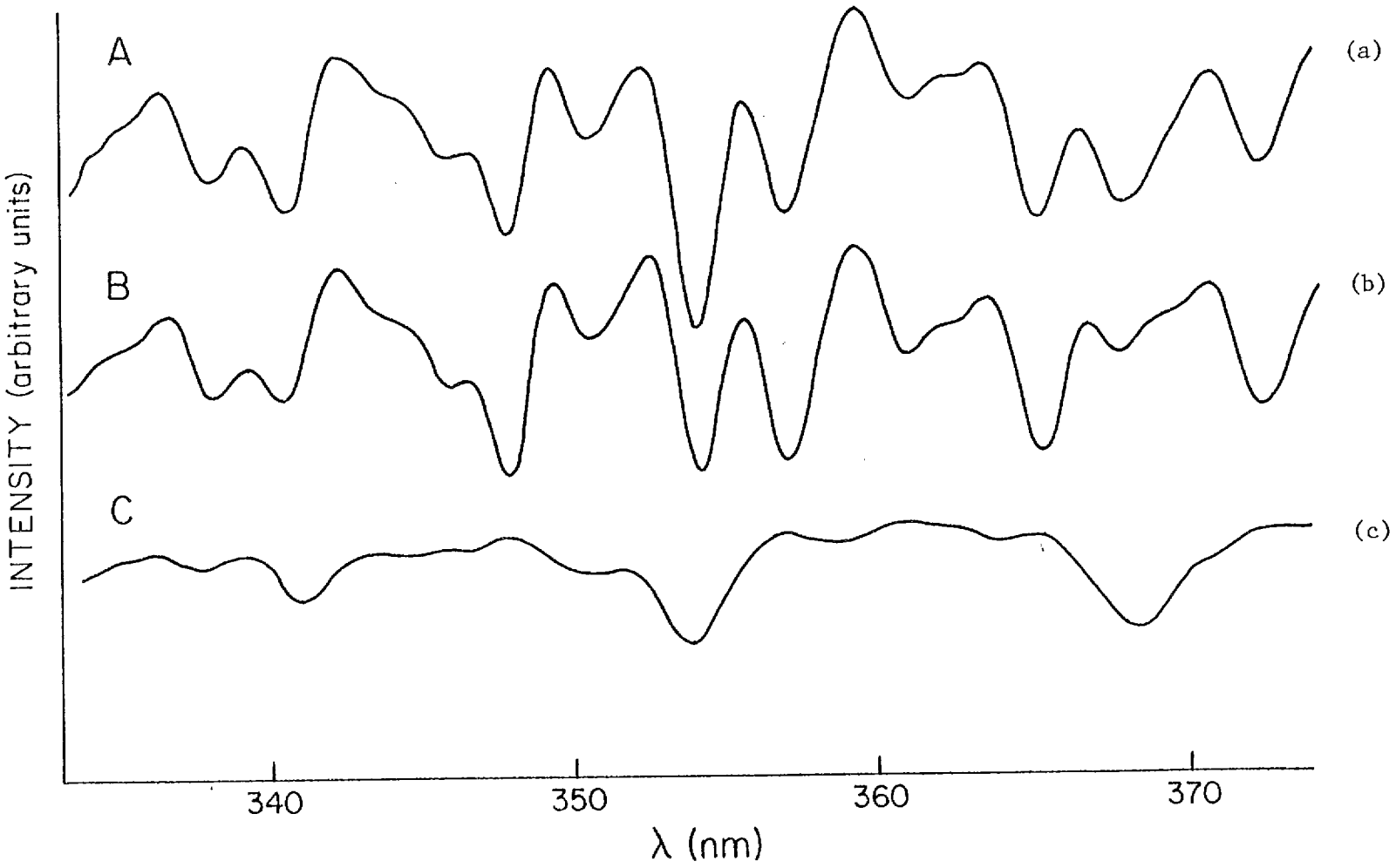

Figure 16. DOAS spectra acquired during phase III (idle) of a loaded mode test of a 1980 Ford F-100 pickup. [a] Spectrum from the CVS system at point C in Figure 2 (page 11); [b] computer-fitted NO_2 spectrum (x4); [c] result of normalized division of (a) by (b) showing features due to HONO.

D. Discussion

While the possible (indeed probable) occurrence of heterogeneous physical and chemical processes on the walls of the CVS train limits the significance of the absolute values observed, certain trends are suggested by these data as discussed below.

1. Concentrations of Nitrous Acid, and Nitrous Acid to Nitrogen Dioxide Ratios

The concentrations of HONO observed in diluted auto exhaust (point C, Figure 2) for vehicles undergoing the standard highway driving cycle (Table 2) ranged from below detection limits (~50 ppb) for certain vehicles (e.g., a 1980 BMW 320i) to ~0.7 ppm for others (e.g., a 1977 Mercury Bobcat). On the other hand, for the high cruise (HC) loaded operating mode (Table 4), much higher HONO levels (and generally higher NO_2 levels) were observed. Thus, with one exception (a 1975 Ford pickup), over 0.5 ppm HONO was measured for each vehicle studied. Maximum HONO observed for this mode was 2.59 ppm for a 1980 Ford Pickup truck.

In all seven vehicles operated using the Cold CVS II mode (Table 3), larger concentrations of HONO and higher ratios of $HONO/NO_2$ were observed in the first phase of this test (cold start, 505 sec cruise) than in phases II and III (862 sec cruise and warm start and 505 sec cruise after a 10-minute soak, respectively). $HONO/NO_2$ ratios ranged from ~0.20 to ~0.40 in phase I and from 0.07 to ~0.20 in phases II and III.

Trends between the three stages of the loaded operating mode test procedure (high cruise, low cruise, idle) were less definitive. For example, a 1980 Mustang produced roughly three times as much HONO and NO_2 at high cruise compared to low cruise, while a turbocharged version of the same vehicle produced twice as much HONO and seven times as much NO_2 at low cruise compared to high cruise.

2. Detection of Formaldehyde

In the Cold CVS II procedure, formaldehyde, when detected, tended to be highest in phase I (the cold start). HCHO was detected in only one loaded mode series, which was performed on the low NO_2 1975 Ford pickup truck referred to above. In this case, HCHO was higher at the high cruise and idle modes compared to the low cruise mode. At this point there is little more to be deduced from the formaldehyde results, other than the

important fact that HCHO can be measured in an on-line manner with our DOAS system. This would be another interesting topic for future study.

3. Dilution and Heterogeneous Reactions in the Sampling System

The relationship of the concentrations observed at point C in the flow tube mode to actual concentrations at the tailpipe (point A) is difficult to estimate from these initial data. This is the case not only because of the possible occurrence of heterogeneous chemistry, but also because the degree of dilution of the exhaust sample before entering the DOAS flow cell could not be accurately judged (i.e., dilution occurring between point A and point C, Figure 2, in addition to air deliberately added).

However, some indication of the degree of dilution can be obtained by comparison of the NO_2 and HONO concentrations for one particular vehicle at the usual sampling point (point C in Figure 2) and at the point at which bag samples were taken for ARB analyses (point B in Figure 2). The dilution factor at the bag-fill point for that run was 5.12; DOAS measurements (Table 5) of the contents of the bag indicated the presence of 67 ppm NO_2 and 8.5 ppm HONO at that point. At point C, DOAS spectra showed 13.4 ppm NO_2 and 1.4 ppm HONO as the exhaust flowed through the flow tube cell. This would suggest an additional dilution of a factor of ~5 occurred when the already diluted (5.12) exhaust passed between these two points. The $HONO/NO_2$ ratio at the two sample points in this pair of runs was roughly constant (0.13 vs. 0.10); however, it is not clear that this generally will be the case if the HONO was at least partially formed from emitted NO_x in heterogeneous reactions proceeding on the surfaces of the sampling train.

The observations of much higher NO_2 levels in the sample bag compared to the flow tube makes it impossible to place great significance on the absolute values of NO_2 and HONO observed in the flow tube mode. They further suggest that heterogeneous NO_x reactions occurred within the CVS system before DOAS analysis and may have been responsible for much of the observed HONO. As noted earlier, exploring this area will be a major focus of the second year program.

4. Contribution of Light Duty Motor Vehicle Exhaust to Ambient Concentrations of Nitrous Acid

At this stage of our research with the shortpath DOAS system, it is not possible to calculate or predict the levels of HONO in the non-diluted exhaust gases immediately leaving the tailpipe (point A, Figure 2) of a LDMV run on the dynamometer-CVS facility. It is also not possible at this time to estimate the levels of HONO present in the exhaust gases emitted by LDMV, for example in freeway traffic. However, these questions should be answered in the next phase of this research project (see below, suggestions of future work).

Certainly, the ambient levels and direct or indirect (i.e., after rapid dilution and cooling by ambient air) emission factors for HONO arising from LDMV (and/or from other NO_x sources) should be known in order to make reliable model calculations of the amounts and rates of ozone production, and other manifestations of photochemical air pollution, in California's heavily polluted air basins. Indeed, totally arbitrary amounts of "initial" HONO often have been used by modelers as adjustable sources of OH radicals when they set the initial conditions for kinetic-computer models of ozone formation in ambient atmospheres.

E. Relevance to Other Research

Analysis of Bag Samples and Smog Chamber Studies. The observation of 8.5 ppm of nitrous acid in a sample bag filled (at point B) by recommended ARB/Federal procedures is of potential importance. The observed formation of HONO should have no significant impact on ARB analyses which are performed promptly after collection. However, as we have seen (Equation 1, page 7), HONO is readily photolyzed by wavelengths $\leq$ 400 nm to produce the OH radical, which then initiates chain photooxidations of hydrocarbons and other organics. Consequently, our results indicate that exhaust samples collected by standard procedures and stored in the light for some period of time before analysis may be subject to considerable photochemical modifications. These could lead, for example, to the formation of significant quantities of aldehydes from nonmethane hydrocarbons in the sample bag and thus give an artifact compared to the true aldehyde concentrations in the freshly-emitted samples.

Other experimental programs (e.g., Dimitriades 1972) have used diluted auto exhaust as the starting material in smog chamber irradiations to investigate oxidant formation. While experiments of this type do not necessarily require a detailed knowledge of the composition of the exhaust gases employed, the assumption is implicit that the gas mix is identical to the freshly emitted effluent from LDMV.

Our new results showing the presence of elevated levels of HONO in sample bags cast some doubt on the validity of that assumption. They raise the possibility that because of the presence of the active photo-initiator HONO, diluted and cooled auto exhaust in smog chambers may be more photo-reactive than "freely emitted" exhaust. However, should HONO form rapidly when hot exhaust gases containing substantial levels of NO_2 and NO are emitted into ambient air, the photo-reactivity of the resulting ambient air parcel (e.g., along a heavily-travelled freeway) may approach that of the diluted exhaust in sample bags and in smog chambers. As noted earlier, experiments are underway in our current ARB program to test this hypothesis.

Health Effects. The presence of significant levels of HONO in the bag samples taken at point B also has potentially significant implications for studies of the effects of dilute auto exhaust on the health of experimental animals. A number of such studies have been conducted in which animals are exposed over periods of time to diluted LDMV exhaust (although at greater dilution ratios) using equipment functionally similar to the ARB/CVS sample bag systems (e.g., Pepelko et al. 1979, Pepelko 1981, Pepelko 1982). Given the high reactivity *in vitro* of nitrous acid toward, for example, secondary amines (Pitts et al. 1978, Tuazon et al. 1978) to produce highly carcinogenic nitrosamines, careful attention should be paid to the probable presence of elevated HONO levels in such exposure systems.

Our preliminary data do not allow the elucidation of the mechanism(s) producing the observed HONO in sampled auto exhaust. However, current research supported by the ARB is designed to measure unambiguously the levels of HONO in LDMV exhaust freely emitted to the atmosphere. If these levels are appreciable, such forthcoming data should be of utility in a variety of areas involving assessments of the health impacts of ambient

HONO. These include, for example, indirect health effects which might be predicted on the basis of airshed modeling of ozone dosages. Thus, we have calculated (Harris et al. 1982) that the presence of predawn levels of 10 ppb HONO in the DTLA atmosphere could lead to significantly elevated ozone dosages at concentrations above California's first stage alert (0.2 ppm for one hour). Clearly, models used to predict the effects of proposed control strategies on ozone dosages, and hence on ozone health impacts, must incorporate realistic ambient HONO levels and estimates of HONO source strengths.

As noted above, a more direct health implication of the presence of HONO in LDMV exhaust emissions is the potential involvement of HONO in the in vivo or in vitro formation of nitrosamines, a highly carcinogenic class of compounds. Thus, while other possible biological responses to inhaled nitrous acid have not been investigated, HONO seems likely to represent a bioavailable source of the nitrite ion.

In this regard, it is interesting (and perplexing) that Pepelko (1981), in summarizing recent EPA-sponsored research concerning possible health effects of exposure to whole diesel exhaust (gases and particles), noted that, while no oncological effects were observed, a variety of non-oncological effects were seen in exposed animals. He concluded these were probably due to certain vapor phase components of the exhaust gases such as aldehydes. The probable presence of nitrous acid in the animal test systems he was discussing, in addition to formaldehyde and acrolein (as well as NO_2 and NO), suggests that investigations into the health effects of (as well as into control strategies for) nitrous acid would seem to be warranted.

F. Recommendations for Future Work

Recommendations include conducting two new experiments, one of which is based on modifications to the present DOAS system. Results from these studies should afford a much better understanding of the magnitude (and hence significance) of the overall contributions by LDMV emissions to observed HONO levels in the atmosphere. Furthermore they should permit an estimation of the ratio of "primary" to "secondary" HONO near a major freeway in the Los Angeles area. The experiments include:

- A longpath DOAS system will be used to make virtually simultaneous measurements of the concentrations of HONO, NO_2, and HCHO along a freeway as a function of time of day, traffic densities and meteorological parameters, especially wind speed, wind direction, relative humidity and temperature.

- A multipass White cell optical system of completely open construction will be designed and constructed. It will be incorporated into the DOAS system and used to monitor the HONO, NO_2 and HCHO levels in the exhaust gases from individual LDMV (including diesels which are high NO_2-emitters). Experiments will be conducted in a manner as free as possible from the potential problems associated with heterogeneous chemistry occurring in the CVS train [e.g., on surfaces between the automobile tailpipe and the sample bag (point B) or exit port of the CVS train (point C)].

III. REFERENCES

Carter, W. P. L., Lloyd, A. C., Sprung, J. L. and Pitts, J. N., Jr. (1979): Computer modeling of smog chamber data: progress in validation of a detailed mechanism for the photooxidation of propene and n-butane in photochemical smog. Inter. J. Chem. Kinet., 11, 45.

Carter, W. P. L., Winer, A. M. and Pitts, J. N., Jr. (1981): Effect of peroxyacetyl nitrate on the initiation of photochemical smog. Environ. Sci. Technol., 15, 831.

Chan, W. H., Nordstrom, R. J., Calvert, J. G. and Shaw, J. H. (1976): Kinetic study of HONO formation and decay reactions in gaseous mixtures of HONO, NO, NO_2, H_2O and N_2. Environ. Sci. Technol., 10, 674.

Cleveland, W. S., Graedel, T. E. and Kleinir, B. (1977): Urban formaldehyde: observed correlation with source emissions and photochemistry. Atmos. Environ., 11, 357.

Dimitriades, B. (1972): Effects of hydrocarbon and nitrogen oxides in photochemical smog formation. Environ. Sci. Technol. 6, 253.

Druckrey, H., Preussman, R., Schmahl, D. and Muller, M. (1961): Chemical constitution and carcinogenic action of nitrosamines. Naturwissenschaffen, 48, 134.

Finlayson-Pitts, B. J. and Pitts, J. N., Jr. (1977): The chemical basis of air quality: kinetics and mechanisms of photochemical air pollution and application to control strategies. Adv. Environ. Sci. Technol., 7, 75.

Goodall, C. M. and Kennedy, T. H. (1976): Carcinogenicity of dimethylnitramine in NZR rats and NZO mice. Cancer Lett., 1, 295.

Hanst, P. L., Wilson, W. E., Patterson, R. K., Gay, B. W., Chaney, L. W. and Burton, C. S. (1975): A spectroscopic study of California smog. EPA Publication No. 650/4-75-006, Environmental Protection Agency, Washington, D. C.

Harris, G. W., Carter, W. P. L, Winer, A. M., Pitts, J. N., Jr., Platt, U. and Perner, D. (1982): Observations of nitrous acid in the Los Angeles atmosphere and implications for predictions of ozone-precursor relationships. Environ. Sci. Technol., in press.

Hendry, D. G. and Kenley, R. A. (1977): The role of peroxyacetylnitrates (PAN) in smog formation. Presented at the 173rd National ACS Meeting, New Orleans, LA, March 20-25, 1977.

Hendry, D. G. and Kenley, R. A. (1979): Atmospheric chemistry of peroxynitrates. In: Nitrogenous Air Pollutants: Chemical and Biological Implications, D. Grosjean, ed., Ann Arbor, MI, p. 137.

Kaiser, E. W. and Wu, C. H. (1977): A kinetic study of the gas phase formation and decomposition reactions of nitrous acid. J. Phys. Chem., 81, 1701.

Komiyama, H. and Inone, H. (1980): Absorption of nitrogen dioxide into water. Chem. Eng. Sci., 35, 154.

Lee, Y. N. and Schwartz, S. E. (1981): Reaction kinetics of nitrogen dioxide with liquid water at low partial pressure. J. Phys. Chem., 85, 840.

Ottolenghi, M. and Rabani, J. (1968): Photochemical generation of nitrogen dioxide in aqueous solutions. J. Phys. Chem., 72, 593.

Pepelko, W. E. (1981): EPA studies on the toxicological effects of inhaled diesel engine emissions. Presented at EPA 1981 Diesel Emissions Symposium, Raleigh, North Carolina, October 5-7, 1981. To be published in Toxicological Effects of Emissions from Diesel Engines, J. Lewtas (Ed.), Elsevier North Holland, Inc.

Pepelko, W. E. (1982): Effects of 28 days exposure to diesel engine emissions in rats. Environ. Res., 27, 16.

Pepelko, W. E., Orthnefer, J. G. and Yang, Y. Y. (1979): Effects of 90 days exposure to catalytically treated automobile exhaust in rats. Environ. Res., 19, 91.

Perner, D. and Platt, U. (1979): Detection of nitrous acid in the atmosphere by differential optical absorption. Geophys. Res. Lett., 6, 917.

Pitts, J. N., Jr. (1982): Formation and fate of gaseous and particulate mutagens and carcinogens in real and simulated atmospheres. Presented at the Karolinska Institute Symposium entitled "Biological Tests in Evaluation of the Mutagenicity and Carcinogenicity of Air Pollutants with Special Reference to Motor Exhausts and Coal Combustion Products," Stockholm, Sweden, February 8-12, 1982. Environ. Health Perspect., accepted for publication.

Pitts, J. N., Jr., Grosjean, D., van Cauwenberghe, K., Schmid, J. P. and Fitz, D. R. (1978): Photooxidation of aliphatic amines under simulated atmospheric conditions: formation of nitrosamines, nitramines, amides and photochemical oxidant. Environ. Sci. Technol., 12, 946.

Pitts, J. N., Jr., Harris, G. W., Winer, A. M., and Treacy, J. J. (1982): Identification and Measurement of Gaseous Nitrous Acid in Dilute Auto Exhaust from a CVS Facility. Environ. Sci. Technol., submitted for publication.

Platt, U., Perner, D. and Patz, H. W. (1979): Simultaneous measurement of atmospheric CH_2O, O_3, and NO_2 by differential optical absorption. J. Geophys. Res., 84, 6329.

Platt, U., Perner, D., Harris, G. W., Winer A. M. and Pitts, J. N., Jr. (1980): Observations of nitrous acid in an urban atmosphere by differential optical absorbtion. Nature, 285, 312.

Sada, E., Kumazawa, H. and Butt, M. A. (1979): Single and simultaneous absorptions of lean SO_2 and NO_2 into aqueous slurries of $Ca(OH)_2$ or $Mg(OH)_2$ particles. J. Chem. Eng., Japan, 12, 111.

Tuazon, E. C., Winer, A. M., Graham, R. A., Schmid, J. P. and Pitts, J. N., Jr. (1978): Fourier transform infrared detection of nitramines in irradiated amine-NO_x systems. Environ. Sci. Technol., 12, 954.

Tuazon, E. C., Winer, A. M., Graham, R. A., Pitts, J. N., Jr. (1980): Atmospheric measurements of trace pollutants by kilometer-pathlength FT-IR spectroscopy. Adv. Environ. Sci. Technol., 10, 259.